iScience

CellPress
OPEN ACCESS

Article

AID-induced CXCL12 upregulation enhances castration-resistant prostate cancer cell metastasis by stabilizing β-catenin expression

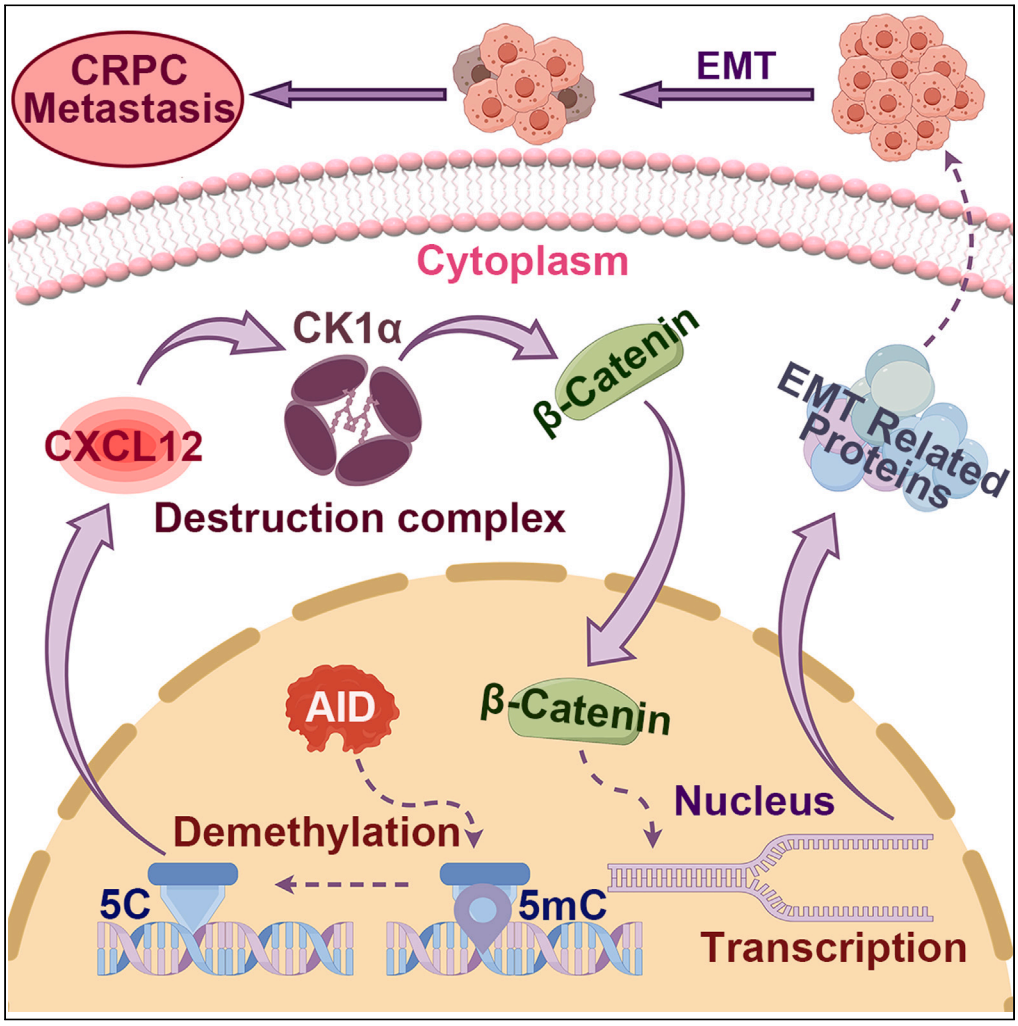

Qi Li, Jinfeng Fan, Zhiyan Zhou, ..., Xiangli Yang, Peiyu Liang, Haoyong Li

xiangli_yang@163.com (X.Y.)
peiyuliang1965@foxmail.com (P.L.)
rm002243@whu.edu.cn (H.L.)

Highlights

AID is aberrantly expressed in prostate cancer tissue and related with ISUP level

AID is highly expressed in CRPC cells and upregulates CXCL12 by demethylation

CXCL12 stabilizing the expression of β-catenin by downregulating CK1α

AID upregulates MMP14 and WLS to facilitate prostate cancer cell metastasis

Li et al., iScience *26*, 108523
December 15, 2023
https://doi.org/10.1016/j.isci.2023.108523

iScience

CellPress
OPEN ACCESS

Article

AID-induced CXCL12 upregulation enhances castration-resistant prostate cancer cell metastasis by stabilizing β-catenin expression

Qi Li,[1,3,5] Jinfeng Fan,[2,5] Zhiyan Zhou,[2,5] Zhe Ma,[4,5] Zhifei Che,[2] Yaoxi Wu,[2] Xiangli Yang,[3,*] Peiyu Liang,[2,*] and Haoyong Li[1,6,*]

SUMMARY

Prostate cancer (PCa) is one of the most common malignant diseases of urinary system and has poor prognosis after progression to castration-resistant prostate cancer (CRPC), and increased cytosine methylation heterogeneity is associated with the more aggressive phenotype of PCa cell line. Activation-induced cytidine deaminase (AID) is a multifunctional enzyme and contributes to antibody diversification. However, the dysregulation of AID participates in the progression of multiple diseases and related with certain oncogenes through demethylation. Nevertheless, the role of AID in PCa remains elusive. We observed a significant upregulation of AID expression in PCa samples, which exhibited a negative correlation with E-cadherin expression. Furthermore, AID expression is remarkably higher in CRPC cells than that in HSPC cells, and AID induced the demethylation of CXCL12, which is required to stabilize the Wnt signaling pathway executor β-catenin and EMT procedure. Our study suggests that AID drives CRPC metastasis by demethylation and can be a potential therapeutic target for CRPC.

INTRODUCTION

Prostate cancer (PCa) is the second most common malignant disease in the male urinary system and ranks second and fifth among the newly increased and leading causes of cancer-related deaths worldwide.[1] Various therapies, including radical resection, chemotherapy, and endocrine therapy, have achieved a certain curative effect on hormone-sensitive prostate cancer (HSPC), whereas the overall survival rate of patients with failed androgen deprivation therapy has dropped. Epigenetic modifications are widely involved in the progression of various cancer types,[2–4] and the (de)methylation of certain genes is crucial for the drug resistance and metastasis of castration-resistant prostate cancer (CRPC).[5,6] However, the molecular mechanism of demethylation that promotes CRPC metastasis remains elusive, and no effective therapeutics that target this pathogenic change has been well explored.

As a versatile enzyme with 198 amino acids, activation-induced cytidine deaminase (AID) is usually expressed in germinal center B cells and acts via somatic hypermutation and class switch recombination by leading to uracil-guanine (U:G) mismatch through the deamination cytosine to uracil; eventually, AID facilitates antibody diversity against pathogen invasion.[7] By contrast, the aberrant expression of AID is associated with a variety of malignant diseases, including urothelial cell carcinoma, lymphoma, and hepatocellular carcinoma.[8–10] Demethylation is one of the most important constituents of epigenetic modification and predominantly occurs at CpG, where it has a vital role in transcription initiation. The mechanism of AID-induced demethylation has gradually been realized through exploration and the most widely accepted pattern is the deamination model: different from AID causes U:G mismatch by deaminating C into U, when AID-induced deaminate occurs at 5-methylcytosine (5-mC), the T:G mismatch would be accumulated and subsequently thymine DNA glycosylase (TDG) work together with activated base excision repair system (BER) to replace T with C, and demethylation is achieved.[11] Although the mechanism by which AID causes demethylation is not fully understood, AID is a well-known contributor to the progression of malignant disease by demethylation. The regulation of AID is complex; inflammatory paracrine signals, including a number of NF-κB-related factors, play a crucial role in the upregulation of AID.[12] Interestingly, the majority of patients with PCa have a history of prostatic hyperplasia and chronic prostatitis; metformin suppresses the castration-induced epithelial-mesenchymal transition (EMT) by downregulating the cyclooxygenase 2/prostaglandin E2 (PGE2)/signal transducer and activator of transcription 3 (STAT3) axis[13] and restraining the inflammation caused by *Trichomonas vaginalis* to reduce the malignant phenotype of PCa cell by blocking certain receptors (such as CXCR1, CXCR2); moreover, the expression levels of

[1]Department of Urology, Renmin Hospital of Wuhan University, Wuhan, Hubei Province, China
[2]Department of Urology, the First Affiliated Hospital of Hainan Medical College, Haikou, Hainan Province, China
[3]Department of Urology, TianYou Hospital affiliated to Wuhan University of Science & Technology, Wuhan, Hubei Province, China
[4]The First Hospital of Tsinghua University, Beijing, China
[5]These authors contributed equally
[6]Lead contact
*Correspondence: xiangli_yang@163.com (X.Y.), peiyuliang1965@foxmail.com (P.L.), rm002243@whu.edu.cn (H.L.)
https://doi.org/10.1016/j.isci.2023.108523

PGE2, NF-κB, and snail are downregulated.[14] Coincidentally, Hyunjoo Lee et al. reported that the Cox-2/PGE2 pathway increases the expression of AID in B cells.[15] These studies imply that AID is likely to be closely related with PCa through inflammation.

In our previous study, iTRAQ-based proteomics analysis revealed that AID silencing induces the suppression of CXCL12 and wntless Wnt ligand secretion mediator (WLS). CXCL12 is a homeostatic pro-inflammation chemokine with a series of meticulous regulation mechanism and is involved in embryonic development under physiological condition. The management of CXCL12 is complex, including NH2-terminal and COOH-terminal truncation, peptidylarginine deiminase-induced citrullination, posttranslational modification,[16] and eye-attracting epigenetic modification.[17] Anja Tolić et al. reported that PARP-1 silencing decreases the methylation level of CXCL12 promoter and results in the upregulation of CXCL12.[17] The dysregulation of CXCL12 has a negative influence on fatal disease, including the enhancement of EMT procedure.[18] CXCL12 is related to the abnormal activation of the MAPK, NF-κB, Wnt/β-catenin, PI3K/AKT, and JAK2/STAT3 signaling pathways to drive cell proliferation, apoptosis, angiogenesis, and EMT in various malignant diseases.[19] Interestingly, both CXCL12 and AID are involved in chronic inflammation and the progression of malignant disease. Therefore, we hypothesize that AID drives the expression of CXCL12 to promote the EMT in CRPC. Unfortunately, the mechanism of AID in the regulation of CXCL12 remains unclear.

Wnt proteins are a group of hydrophobic glycoproteins with the posttranslational modification of palmitate bond to an N-terminal cysteine or that of palmitoleic acid bond to a cysteine and are pasted on cell membranes tightly.[20] Similar to G-protein-coupled receptors, WLS is a multi-channel transmembrane protein that shuttles among endoplasmic reticulum, Golgi, and plasma membrane to facilitate the intercellular diffusion of Wnts.[21] Wnt proteins are arrested in Wnt-producing cells under WLS suppression.[22] Canonical Wnt pathway (Wnt/β-catenin) plays a crucial role in embryogenesis and organogenesis, whereas the disorder of Wnt/β-catenin pathway exacerbates a large amount of disease and is best known in cancer.[23] As the executor of canonical Wnt signaling pathway, β-catenin induction is regulated by the phosphorylation and ubiquitination caused by destruction complex. Wnt ligand deficiency leads to the formation of multiprotein destruction complex that contains disheveled protein, glycogen synthase kinase 3 beta (GSK3β), casein kinase 1α (CK1α), adenomatous polyposis coli, and axin and phosphorylates intracytoplasmic β-catenin at certain threonine and serine residues for ubiquitination; the next proteasome is employed for the initial degradation of β-catenin.[24] On the contrary, Wnt ligand is co-excitated with Frizzled and low-density lipoprotein receptor-related protein (LPR5/6 receptors) to block the formation of destruction complex. Subsequently, stabilized β-catenin (free of degradation caused by proteasome) is translocated into the nucleus and replaces inhibitor of T cell-specific transcription factor/lymphoid enhancer binding factor to regulate the expression of related downstream genes.[25] Existing evidence suggests that the ectopic activation of Wnt/β-catenin causes off-target phenomenon on downstream genes and cancer metastasis. For instance, Ipsita Pal and colleagues reported that β-catenin facilitates colorectal carcinoma metastasis by promoting EMT progression.[26] Interestingly, existing research revealed that UV radiation upregulates inflammation through the activation of the COX-2/PEG2 axis to stabilize the expression of β-catenin and finally facilitate skin carcinogenesis.[27] A recent study indicated that CXCL12 cross-talks with Wnt/β-catenin to benefit the progression of liver fibrosis.[28] These evidences strongly suggest that AID is involved in the activation of Wnt/β-catenin; however, the underpinning mechanism, especially in PCa, still needs to be further investigated.

In this study, we demonstrated that AID is a crucial administrator of CRPC cell metastasis by upregulating CXCL12 through demethylation and stabilizing the expression of β-catenin to drive the expression of EMT-related proteins. Moreover, we also found that AID promotes the expression of matrix metallopeptidase14 (MMP14) and WLS to facilitate CRPC and HSPC metastasis through non-demethylation method. Our findings suggest that AID is a potential therapeutic target of CRPC.

RESULTS

AID is negatively related to E-cadherin expression in human PCa tissue

Based on existing evidence and our previous study, AID promotes the progression of various malignant diseases by activating the EMT process. Hence, we compared the expression of AID and E-cadherin between PCa with metastasis (mPCa), PCa, prostatic hyperplasia with chronic inflammation (PHCI), and normal prostate (NP) specimens. Expectedly, the expression of AID in mPCa tissue was remarkably higher than those in the other three groups, and expression of AID in PCa tissue is significantly higher than that in PHCI and NP group (Figures 1A and 1B [a, d, g and j]). Interestingly, PHCI tissue expresses AID stronger than NP tissue significantly (Figures 1A and 1B [g and j]). Consistent with the headstream of most PCa cells, AID is located in glandular epithelium cells. Subsequently, we further analyzed the subcellular localization of AID and found that its localization is quite different among (m)PCa, PHCI, and NP tissues. Previous research indicated that AID is more likely degraded in the nucleus on account of heat shock protein deficiency, which protects tissues from mutation- or demethylation-induced cancerization. However, the accumulation of AID in nucleus was remarkably increased in (m)PCa tissue, and interestingly, nuclear AID was observed in PHCI but not in NP (Figures 1A and 1B [i and l]). These observations suggest that AID is incompetent in NP tissue and potentially establishes the connection between inflammation and cancerization in prostate tissue.

Subsequently, we measured the expression of EMT-related protein E-cadherin, which regulates cell adherence. Different from the expression of AID, E-cadherin was downregulated in (m)PCa tissues compared with PHCI and NP (Figures 1C and 1D). Coincidentally, consistent with the location of AID in (m)PCa tissue, E-cadherin was located in the glandular epithelium of NP tissue. Furthermore, the gene expression profiles of 370 PCa specimens (GSE21034) were used to perform gene correlation analysis. We found that AID expression shows a negative correlation with E-cadherin. We divided the data into four groups by Gleason score. An obvious escalating trend in absolute R value was observed with the increase in Gleason score (Figures 1E and 1F). Next, we measured the expression of AID and E-cadherin in NP, PHCI, and (m)PCa tissues with different ISUP (ISUP is short for International Society of Urological Pathology, a brand new Gleason score-based rating system for prostate cancer) level. We found remarkable difference in the expression of AID in NP and PHCI tissues, whereas the same result

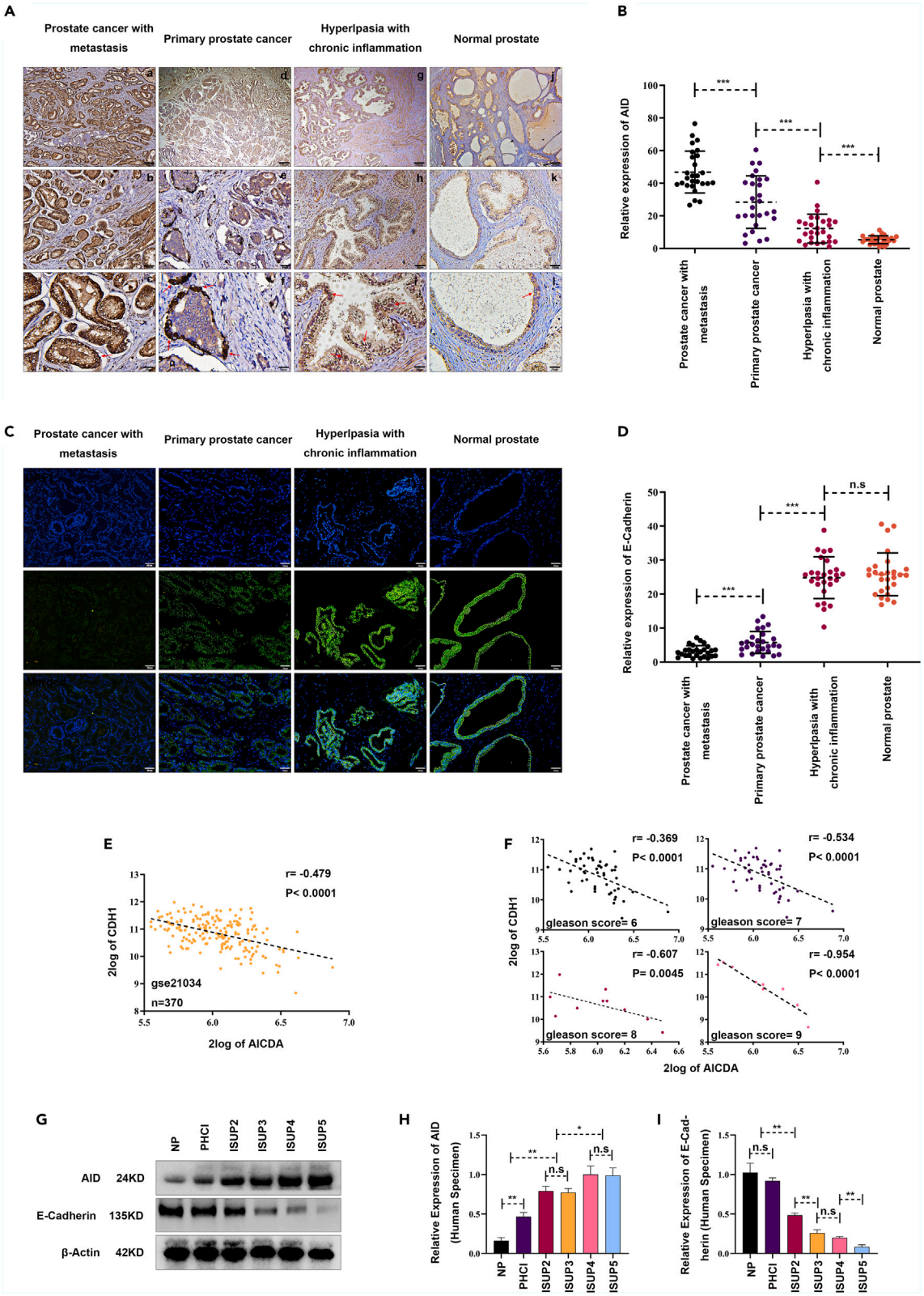
A
Prostate cancer with metastasis
Primary prostate cancer
Hyperlpasia with chronic inflammation
Normal prostate
B
Relative expression of AID
Prostate cancer with metastasis
Primary prostate cancer
Hyperlpasia with chronic inflammation
Normal prostate
C
Prostate cancer with metastasis
Primary prostate cancer
Hyperlpasia with chronic inflammation
Normal prostate
D
Relative expression of E-Cadherin
n.s
E
2log of CDH1
r= -0.479
P< 0.0001
gse21034
n=370
2log of AICDA
F
2log of CDH1
r= -0.369
P< 0.0001
gleason score= 6
r= -0.534
P< 0.0001
gleason score= 7
r= -0.607
P= 0.0045
gleason score= 8
r= -0.954
P< 0.0001
gleason score= 9
2log of AICDA
G
NP
PHCI
ISUP2
ISUP3
ISUP4
ISUP5
AID 24KD
E-Cadherin 135KD
β-Actin 42KD
H
Relative Expression of AID (Human Specimen)
I
Relative Expression of E-Cadherin (Human Specimen)

Figure 1. AID is negatively related to E-cadherin expression in human PCa tissue

(A and B) IHC of AID in human mPCa, PCa, PHCI, and NP specimens. The expression of AID in (m)PCa and PHCI tissue is significantly higher than that in NP tissue ($p < 0.001$, $p < 0.001$, respectively) and in (m)PCa tissue is significantly higher than that in PHCI tissue ($p < 0.001$), and the expression of AID in mPCa tissue is significantly higher than that in PCa tissue. ($p < 0.001$). The red arrow points to expression of AID in nucleus. Scale bar, 200, 50, or 20 μm.

(C and D) Immunofluorescence staining of E-cadherin in human mPCa, PCa, PHCI, and NP specimens. The expression of E-cadherin in PHCI and NP tissue is significantly higher than that in (m)PCa tissue ($p < 0.001$, $p < 0.001$, respectively) and there is no significantly difference between PHCI and NP tissue ($p = 0.56$). Scale bar, 100 μm.

(E and F) The gene correlation analysis between AICDA and CDH1 (encoding E-cadherin) based on database GSE21034. Pearson r values are used to indicate the correlation level. The overall Pearson R value between AICDA and CDH1 is −0.479 ($p < 0.001$), and in Gleason score 6, 7, 8, and 9 group is −0.369, −0.534, −0.609, and −0.954, respectively ($p < 0.001$, $p < 0.001$, $p < 0.01$, $p < 0.001$, respectively).

(G–I) The relative expression of AID and E-cadherin in human PCa tissue. The specimens are distinguished by ISUP level. Overall, the expression of AID in PCa tissue is significantly stronger than that in PHCI and NP tissue. The expression of AID in ISUP 4 and ISUP 5 is significantly higher than that in ISUP 2 and ISUP 3 ($p < 0.05$, <0.05, <0.05, <0.05, respectively), and there is no significant difference between ISUP 2 and ISUP 3 ($p = 0.6845$), or ISUP 4 and ISUP 5 ($p = 0.8915$). The expression of E-cadherin is significantly decreased with the increase of ISUP level, except ISUP 3 and ISUP 4 ($p = 0.0814$). All the experiments were repeated three times. Two-sided Student's *t* test was used for A–D and G–I, Pearson correlation coefficient was used for E and F. *$p < 0.05$, **$p < 0.01$, ***$p < 0.001$, n.s, no significance.

was not observed for the expression of E-cadherin (Figures 1G and 1I). Furthermore, no statistical difference was observed between the expression of AID in tissues with ISUP level 2 and 3. However, the expression of E-cadherin in tissues with ISUP 2 was significantly higher than those with ISUP 3. Furthermore, there is no significant difference of AID expression between ISUP 4 and ISUP 5. However, the E-cadherin expression remarkably downregulated with increased ISUP level (except ISUP 3 and ISUP4). These results indicated that AID is involved in the metastasis of PCa and the correlation between AID and E-cadherin is probably not only dose dependent.

AID upregulates the invasiveness of PCa cells *in vitro*

Various PCa cell lines, including C4-2, C4-2B, PC-3, DU145, 22RV1, and LNCaP, were used to explore the relative expression of AID on the protein level. According to origins from the same lineage and those with relatively higher or lower expression of AID than other cell lines (Figures 2A and 2B), C4-2, C4-2B, and LNCaP were selected for the following experiment. Next, we compared the expression of a couple of EMT-related proteins, including CXCL12, E-cadherin, N-cadherin, vimentin, MMP14, and WLS, in these three prostate cancer cell lines. Expectedly, the expression of these proteins in C4-2 and C4-2B cells was remarkably higher than those in LNCaP cells, except E-cadherin (Figures 2C–2E). Subsequently, transwell assay was used to compare the invasiveness of C4-2, C4-2B, and LNCaP. C4-2 and C4-2B had a more aggressive phenotype than LNCaP (Figures 2F and 2G). The lentivirus-based specific short hairpin RNA (shRNA) of AICDA was designed to downregulate the protein expression of AID, and the shRNA with the best inhibition rates was used in the subsequent experiments (Figures S1A and S1B). Inhibition rates of 83.5%, 81.5%, and 53% were observed in C4-2, C4-2B, and LNCaP cells, respectively (Figures 2H and 2I). Next, the expression levels of CXCL12, N-cadherin, E-cadherin, and vimentin in C4-2, C4-2B, and LNCaP cell lines were measured. The expression of the proteins described previously was considerably suppressed in C4-2 and C4-2B cells under AID silencing (Figures 2J–2L), whereas only MMP14 and WLS were downregulated by AID silencing in LNCaP cells (Figures 2M and 2N). These results indicate that AID promotes EMT process in CRPC cell but not in HSPC cell. Transwell assay was performed to explore the influence of AID on the invasiveness of C4-2, C4-2B, and LNCaP cells. The invasiveness of C4-2 and C4-2B cells was suppressed (Figures 2O and 2P). Furthermore, AID silencing also inhibited the proliferation and migration of C4-2, C4-2B, and LNCaP cells (Figures S2A–S2E). Although the expression of CXCL12, N-cadherin, E-cadherin, and vimentin was not affected by AID knockdown, AID silencing inhibited the invasiveness of LNCaP cells (Figures 2O and 2R).

Taken together with the molecular function of AID and experiment results, we consider that AID participates in EMT procedure in CRPC cells and potentially plays a role in the advancement of PCa to CRPC.

AID enhances the malignant phenotype of C4-2B cells *in vivo*

C4-2B had the most malignant phenotype among the three PCa cell lines; thus, it was used in the animal experiments to explore the impact of AID on CRPC cell *in vivo*. AID silencing substantially decreased the proliferation of C4-2B cells in nude mice. Tumor volume (in mm^3) was calculated by the formula, 0.5 × (long diameter) × (short diameter)^2. The mice were killed by CO_2 overdose transiently after 14 days, and the isolated lump body was used to perform immunohistochemistry (IHC) assay. The tumor volume of the shCon group was obviously larger than the shAICDA group (Figures 3A and 3B). Subsequently, the isolated solid tumor tissue was used to measure the expression of AID, CXCL12, E-cadherin, N-cadherin, vimentin, MMP14, and WLS; IHC staining shows that the expression of target proteins described previously in the shCon group was considerably higher than that in the shACIDA group, and the expression of E-cadherin is conversely (Figures 3C and 3D). Besides, consistent with the IHC of human (m)PCa specimen, AID was more highly expressed in the nucleus of tumor cell in the shCon group than that in the shAICDA group (Figures 1A, 1B, 3C, and 3D).

In the metastatic assay, AID silencing obviously inhibited the metastasis of C4-2B cells. In the negative control group, the number of metastatic tumors in nude mice lung was evidently much more than that in the AID silencing group (Figures 3E and 3F). Furthermore, IHC assay was performed to observe the order of severity of intrapulmonary metastases and the expression level of AID, CXCL12, E-cadherin,

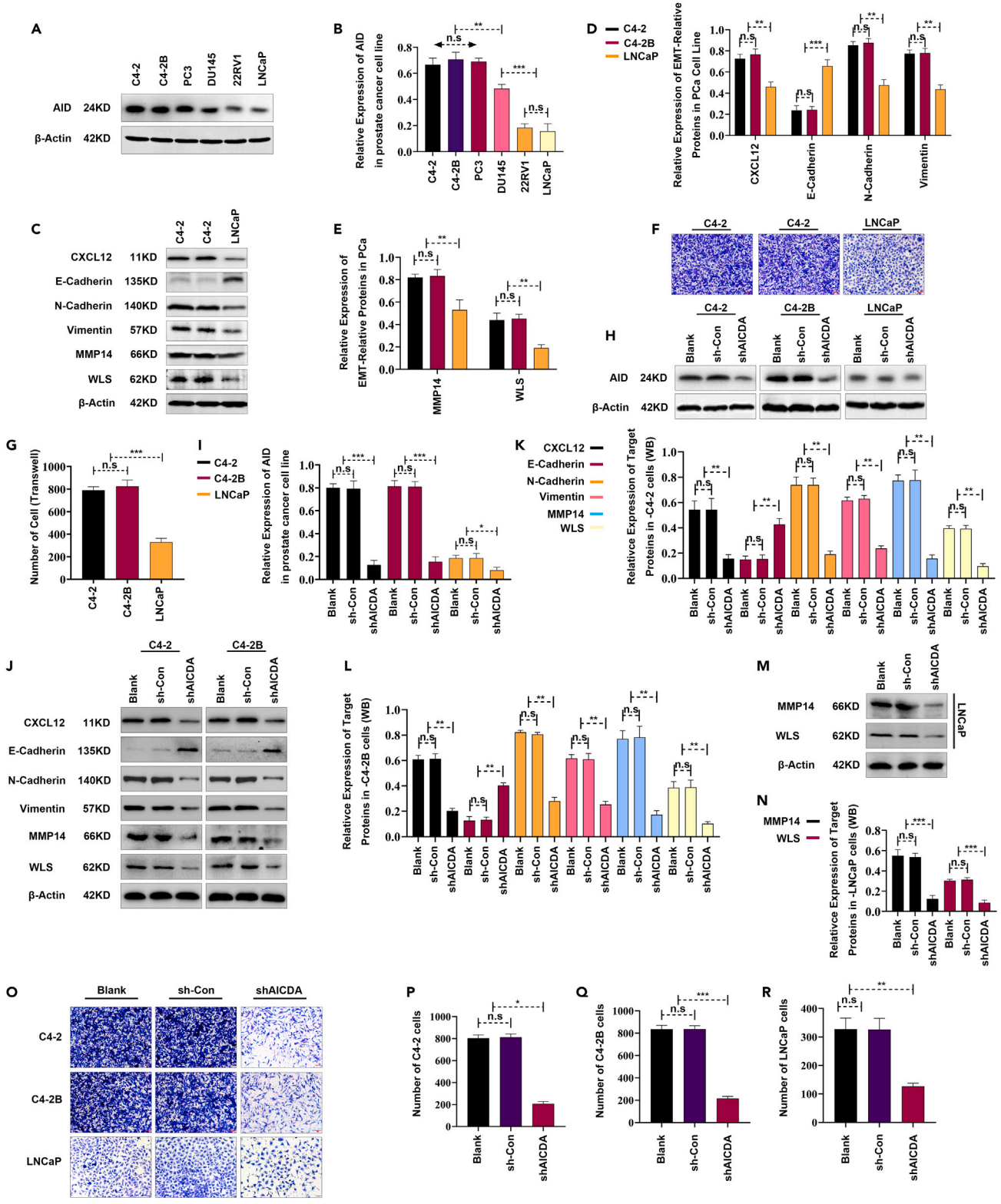
A
C4-2
C4-2B
PC3
DU145
22RV1
LNCaP
AID 24KD
β-Actin 42KD
B
Relative Expression of AID in prostate cancer cell line
C4-2
C4-2B
PC3
DU145
22RV1
LNCaP
D
C4-2
C4-2B
LNCaP
Relative Expression of EMT-Relative Proteins in PCa Cell Line
CXCL12
E-Cadherin
N-Cadherin
Vimentin
C
C4-2
C4-2
LNCaP
CXCL12 11KD
E-Cadherin 135KD
N-Cadherin 140KD
Vimentin 57KD
MMP14 66KD
WLS 62KD
β-Actin 42KD
E
Relative Expression of EMT-Relative Proteins in PCa
MMP14
WLS
F
C4-2
C4-2
LNCaP
H
C4-2
C4-2B
LNCaP
Blank
sh-Con
shAICDA
AID 24KD
β-Actin 42KD
G
Number of Cell (Transwell)
C4-2
C4-2B
LNCaP
I
C4-2
C4-2B
LNCaP
Relative Expression of AID in prostate cancer cell line
Blank
sh-Con
shAICDA
K
CXCL12
E-Cadherin
N-Cadherin
Vimentin
MMP14
WLS
Relative Expression of Target Proteins in -C4-2 cells (WB)
J
C4-2
C4-2B
Blank
sh-Con
shAICDA
CXCL12 11KD
E-Cadherin 135KD
N-Cadherin 140KD
Vimentin 57KD
MMP14 66KD
WLS 62KD
β-Actin 42KD
L
Relative Expression of Target Proteins in -C4-2B cells (WB)
M
Blank
sh-Con
shAICDA
MMP14 66KD
WLS 62KD
β-Actin 42KD
LNCaP
N
MMP14
WLS
Relative Expression of Target Proteins in -LNCaP cells (WB)
O
Blank
sh-Con
shAICDA
C4-2
C4-2B
LNCaP
P
Number of C4-2 cells
Blank
sh-Con
shAICDA
Q
Number of C4-2B cells
Blank
sh-Con
shAICDA
R
Number of LNCaP cells
Blank
sh-Con
shAICDA

Figure 2. AID upregulates the invasiveness of PCa cells *in vitro*

(A and B) The expression of AID in prostate cancer cell lines. Overall, the expression of AID in CRPC cells is significantly higher than that in HSPC cells. There is no significant difference of AID expression between C4-2, C4-2B, and PC3 cells ($p = 0.4057$, 0.5165, and 0.6612, respectively), or between 22RV1 and LNCaP cells ($p = 0.5185$).

(C–E) The expression of CXCL12, E-cadherin, N-cadherin, vimentin, MMP14, and WLS in experimental cell lines. The EMT-related proteins described above express significantly higher in CRPC cells than that in androgen-sensitive prostate cancer cells ($p < 0.01$); conversely, the expression of E-cadherin in HSPC cells is significantly higher than that in CRPC cells ($p < 0.001$), and the expression of those proteins has no significant difference between C4-2 and C4-2B cells ($p > 0.05$).

(F and G) Transwell assay shows that the invasiveness of C4-2 and C4-2B cells is significantly stronger than that in LNCaP cells ($p < 0.001$), and there is no significant difference between C4-2 and C4-2B cells ($p = 0.4138$).

(H and I) The lentivirus-based AICDA-specific shRNA significantly inhibits AID expression in all three experimental cell lines (C4-2 and C4-2B: $p < 0.001$; LNCaP: $p < 0.05$, respectively).

(J–L) AICDA silencing significantly downregulates CXCL12, N-cadherin, vimentin, MMp14, and WLS and upregulates E-cadherin in C4-2 and C4-2B cell ($p < 0.01$).

(M and N) The expression of MM14 ($p < 0.001$) and WLS ($p < 0.001$) in LNCaP cells is significantly inhibited by AICDA silencing.

(O–R) Transwell assay shows that shAICDA significantly suppresses the invasiveness of C4-2 ($p < 0.05$), C4-2B ($p < 0.001$), and LNCaP cells ($p < 0.01$). Scale bar, 50 μm. Student's *t* test or one-way ANOVA was used to evaluate statistical differences, and data are presented as the means ± standard deviation, all experiments were repeated three times. Two-sided Student's *t* test was used for all panels. *$p < 0.05$, **$p < 0.01$, ***$p < 0.001$, n.s, no significance.

N-cadherin, vimentin, MMP14, and WLS in metastatic tumor. As expected, all metastatic tumors express target proteins strongly, except E-cadherin (Figures 3F–3H). Moreover, the nests of neoplastic cells in both groups expressed AID in the nucleus strongly (Figures 3G and 3H).

Furthermore, another two group of metastatic module mice (n = 17) were used in survival time assay. The autopsy-dependent approach demonstrated that all the experimental mice died from metastatic tumor-induced respiratory failure or pulmonary vascular rupture (Figure 3I) and AID silencing remarkably increased the lifespan of nude mice. The median survival time of the shCon and shAICDA groups was 18.311 and 10.349 days ($p < 0.01$), respectively (Figure 3J). These results suggested that AID is required for the proliferation and metastasis of C4-2B cells *in vivo*, and the suppression of AID prolongs the life cycle of nude mice.

5-Aza-2′-deoxycytidine antagonizes the downregulation of CXCL12 and the invasiveness of CRPC cells caused by AID silencing

5-Aza was used to explore the potential mechanism of AICDA silencing-induced downregulation of CXCL12. 5-Aza significantly promotes the expression of CXCL12 on protein level in all experimental cell lines; interestingly, AID silencing was not inhibited by the CXCL12 expression in LNCaP cell line (Figures 4A and 4B).

The lentivirus-based specific shRNA of CXCL12 was designed to downregulate the protein expression of CXCL12, and the shRNA with the best inhibition rates was used in the subsequent experiments (Figures S3A and S3B). Furthermore, CXCL12 silencing was not influenced by the expression of AID in C4-2, C4-2B, and LNCaP cell line (Figures 4C and 4D), and AID silencing obviously depressed the CXCL12 transcription in C4-2 and C4-2B cell lines, whereas the same result was not observed in LNCaP cells (Figure 4E). These results suggested that AID-induced demethylation modification regulates the CXCL12 expression unidirectionally in C4-2 and C4-2B cell lines. Moreover, to validate if CXCL12 is the footstone of AID silencing-induced depression of invasiveness in C4-2 and C4-2B cell line, 5-aza was used to treat the CXCL12-silenced C4-2, C4-2B, and LNCaP cell lines. CXCL12 silencing significantly upregulated E-cadherin and downregulated N-cadherin and vimentin in C4-2 and C4-2B cell lines, and 5-aza neither counter the upregulation of E-cadherin nor downregulation of N-cadherin and vimentin (Figures 4F and 4G); however, both CXCL12 silencing and 5-aza was incapable of regulating the expression of E-cadherin, N-cadherin, and vimentin in LNCaP cells. Moreover, 5-aza significantly converted the AICDA silencing-induced upregulation of E-cadherin and downregulation of N-cadherin and vimentin in C4-2 and C4-2B cells, and consistent with the experiment result described previously, the expression of E-cadherin, N-cadherin, and vimentin in LNCaP cells was not influenced by the AICDA silencing (Figures 4H–4K). Then, the specific overexpression sequence of AICDA was employed to upregulate AID in C4-2 and C4-2B cells (Figures S4A–S4D). However, AID overexpression failed to upregulate N-cadherin and vimentin or downregulate E-cadherin in CXCL12 silenced in C4-2 and C4-B cells (Figures 4L–4N). These results indicated that expression of EMT-related proteins including E-cadherin, N-cadherin, and vimentin was not affected by demethylation modification directly in C4-2 and C4-2B cell line, and CXCL12 is indispensable for AID-induced EMT process in C4-2 and C4-2B cells. Besides, consistent with the AICDA silencing group, transwell assay showed that the invasiveness of C4-2 and C4-2B cells was also downregulated by CXCL12 silencing; 5-aza converts the AICDA silencing-induced invasiveness depression in C4-2 and C4-2B cells; however, the same result was not observed in CXCL12-silenced group (Figures 4O and 4P). These results suggested that demethylation is incapable of enhancing the invasiveness of CXCL12-silenced C4-2 and C4-2B cells and further confirmed that CXCL12 is an irreplaceable relay station in AID-induced invasiveness upregulation of C4-2 and C4-2B cells. In addition, overexpression of AID failed to recover the CXCL12 silencing-induced expression variation of E-cadherin, N-cadherin, and vimentin, whereas transwell assay showed that overexpression of AID partially recovered the CXCL12 silencing-induced invasiveness depression of C4-2 and C4-2B cells, and this phenomenon indicated that some other factors are also involved in the AID-induced invasiveness upregulation of C4-2 and C4-2B cells.

CXCL12 is positively related to the Wnt/β-catenin signaling pathway and promotes the EMT process in malignant disease. Thus, correlation analysis was performed between CXCL12 and the vital factors of the Wnt/β-catenin pathway in multiple databases, including CSNK1A1 (encoding CK1α), GSK3β, and CTNNNB1 (encoding β-Catenin). We found that the transcription of CXCL12 is negatively related to β-catenin

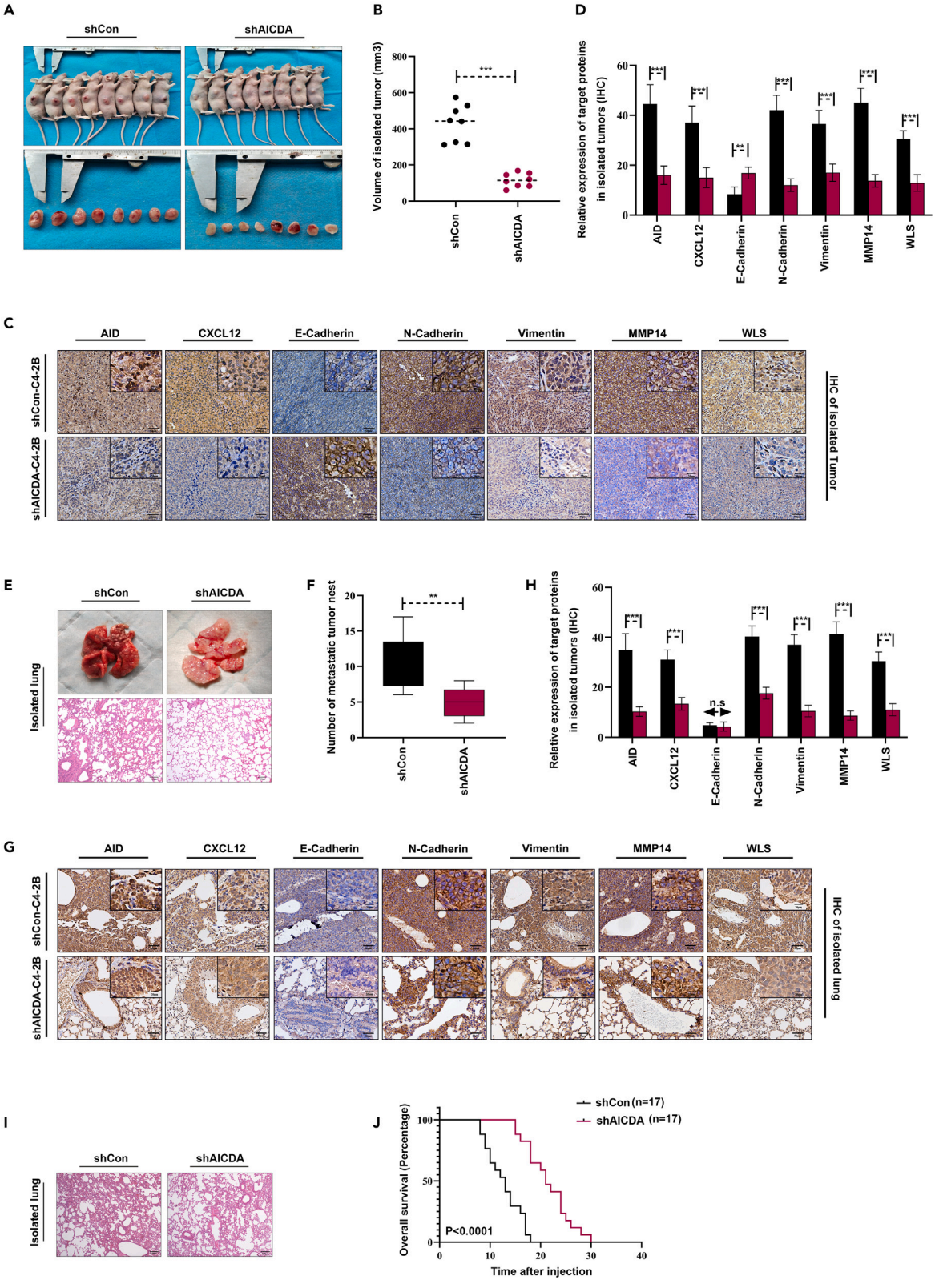
A
shCon
shAICDA
B
Volume of isolated tumor (mm3)
800
600
400
200
0
***
shCon
shAICDA
D
Relative expression of target proteins in isolated tumors (IHC)
60
40
20
0
***
**
AID
CXCL12
E-Cadherin
N-Cadherin
Vimentin
MMP14
WLS
C
AID
CXCL12
E-Cadherin
N-Cadherin
Vimentin
MMP14
WLS
shCon-C4-2B
shAICDA-C4-2B
IHC of isolated Tumor
E
shCon
shAICDA
Isolated lung
F
Number of metastatic tumor nest
20
15
10
5
0
**
shCon
shAICDA
H
Relative expression of target proteins in isolated tumors (IHC)
60
40
20
0
***
n.s
AID
CXCL12
E-Cadherin
N-Cadherin
Vimentin
MMP14
WLS
G
AID
CXCL12
E-Cadherin
N-Cadherin
Vimentin
MMP14
WLS
shCon-C4-2B
shAICDA-C4-2B
IHC of isolated lung
I
shCon
shAICDA
Isolated lung
J
shCon (n=17)
shAICDA (n=17)
Overall survival (Percentage)
100
50
0
P<0.0001
0
10
20
30
40
Time after injection

Figure 3. AID enhances the malignant phenotype of C4-2B cells *in vivo*

(A and B) AICDA silencing significantly suppresses the proliferation of C4-2B cells in nude mice ($n = 8$, $p < 0.001$). Tumor volume (in mm^3) was calculated by the formula, 0.5 × (long diameter) × (short diameter)^2.

(C and D) IHC shows that AID, CXCL12, N-cadherin, vimentin, MMP14, and WLS expression is significantly higher in shCon group than that in shAICDA group, and expression of E-cadherin is conversely ($n = 8$, $p < 0.01$). Scale bar, 50 or 20 μm.

(E and F) The number of metastatic tumor in shCon group is significantly much more than that in shAICDA group ($n = 8$, $p < 0.01$). (G and H) IHC shows that the expression of AID, CXCL12, N-cadherin, vimentin, MMP14, and WLS in shCon group is significantly higher than that in shAICDA group ($p < 0.001$), and there is no significant difference of E-cadherin expression level between both group ($p > 0.05$), and almost all metastatic cancer cells express target proteins strongly, except E-cadherin. Scale bar = 100 or 50 μm.

(I) HE staining of experimental mice lung shows that all nude mice used in survival time analysis die of C4-2B cell-induced pulmonary alveoli or blood vessel destruction. Scale bar, 100 μm.

(J) The Kaplan-Meyer curve was performed to explore the influence caused by AID on survival time of nude mice. AICDA silencing significantly prolongs the survival time of nude mice ($n = 17$, $p < 0.001$). Two-sided Student's *t* test was used for A and B and E and F, one-way ANOVA was used for C and D and G and H, log rank was used for J, *$p < 0.05$, **$p < 0.01$, ***$p < 0.001$, n.s, no significance.

suppressor CSNK1A1 (GSE46691) (Figure 4Q) and positively related to CTNNB1 under biochemical recurrence condition (according to The Cancer Genome Atlas, Figure 4R). Furthermore, the negative correlation was also established between AICDA and CSNK1A1 based on GSE46691 (Figure S5A). However, the remarkable correlation between CXCL12 and GSK3β was not observed based on the databases (Figures S5B–S5D). In conclusion, AID promotes EMT process by regulating the expression of CXCL12 unidirectionally through demethylation in C4-2 and C4-2B cells.

AID-induced upregulation of CXCL12 stabilizes β-catenin to enhance EMT by inhibiting CK1α in CRPC cells

As the core factor of the WNT pathway, the stability of β-catenin plays a crucial rule in the EMT procedure of malignant diseases. However, phosphorylated β-catenin is apt to undergo ubiquitination and result in degradation. Hence, the expression of the component of destruction complex CK1α was measured to understand the underlying mechanism of AID-induced EMT in C4-2 and C4-2B cells. We found that CK1α was upregulated in the shAICDA and shCXCL12 groups (Figures 5A–5C), and the expression of CK1α was not influenced by 5-aza (Figures S6A–S6C). Subsequently, the expression of β-catenin and pS45-β-catenin/pS33-pS37-Thr41-β-catenin was measured in C4-2 and C4-2B cells under AID or CXCL12 knockdown. β-Catenin was remarkably suppressed, and the expression of pS45-β-catenin and pS33/pS37/Thr41-β-catenin was upregulated (Figures 5D–5H). The pS45-β-catenin is necessary for the GSK3β-induced phosphorylation of β-catenin (pS33/pS37/T41-β-catenin); thus, CXCL12 enhances the expression of β-catenin by blocking the destruction complex-based phosphorylation chain through repressing the expression of CK1α. Subsequently, β-catenin inhibitor pyrvinium, which is specific activator of CK1α, was employed to further substantiate the mechanism of AID-induced EMT in C4-2 and C4-2B cells. Treatment with pyrvinium at appropriate concentration (5 μM) and time(48 h)(Figures S7A and S7B) remarkably upregulated the expression of pS45-β-catenin and pS33/pS37/T41-β-catenin and downregulated β-catenin (Figures 5I–5O). Additionally, no remarkable difference was found among the shAICDA, shCXCL12, and shCon + pyrvinium groups. ShAICDA+shCXCL12 failed to further reduce the expression of β-catenin, and the upregulation of pS45-β-catenin and pS33/pS37/T41-β-catenin was also not observed (Figures 5I–5O).

Moreover, the expression of E-cadherin, N-cadherin, and vimentin was also measured under the experiment condition described previously and compared with the influence on the expression of β-catenin with or without phosphorylation. Pyrvinium caused the similar result in these proteins (Figures 5I–5O). The results suggest that these EMT-related proteins are regulated by AID indirectly through β-catenin in C4-2 and C4-2B cell. Next, transwell assay was performed to test the influence of pyrvinium on the invasiveness of C4-2 and C4-2B cells. No remarkable difference was observed among the shAICDA, shCXCL12, shAICDA + shCXCL12, and shCon + pyrvinium group, and the experimental data of shCon + DMSO group were obviously higher than those of the other groups (Figures 5P–5R).

Furthermore, the expression of pS45-β-catenin and pS33-pS37-Thr41-β-catenin was measured under AID induction in CXCL12-silenced C4-2 and C4-2B cells. Consistent with the result in Figure 4I, AID overexpression failed to manage the expression of pS45-β-catenin and pS33-pS37-Thr41-β-catenin without the assistance of CXCL12 in C4-2 and C4-2B cells (Figures 5S–5U). In summary, AID promotes the EMT process by stabilizing β-catenin through the demethylation of CXCL12.

AID facilitates the metastasis of PCa cells by upregulating MMP14 and WLS

The expression of MMP14 and WLS was measured on the protein level in C4-2, C4-2B, and LNCaP cell lines. AICDA silencing significantly suppressed the MMP14 expression in all experimental cell lines, and 5-aza partially recover the AICDA silencing-induced inhibition of MMP14 in C4-2 and C4-2B cells (Figures 6A and 6B). Besides, CXCL12 silencing significantly suppressed the MMP14 expression in C4-2 and C4-2B cells and overexpression of AID partially recover the CXCL12 silencing-induced MMP14 inhibition, and 5-aza failed to recover the CXCL12 silencing-induced MMP14 inhibition (Figures 6C–6E). Moreover, overexpression of AID significantly upregulated the expression of MMP14 in LNCaP cells; however, neither CXCL12 silencing nor 5-aza influenced the MMP14 expression (Figures 6C–6E). These results suggested that AID-CXCL12 axis was participated in the MMP14 regulation in C4-2 and C4-2B cells; however, AID also regulated MMP14 through pathways other than demethylation. In addition, CXCL12 or AID-induced demethylation was incapable of regulated MMP14 expression in LNCaP cells. These results exactly explain the experimental result in Figure 4O, that is, AID silencing suppresses the invasiveness of LNCaP

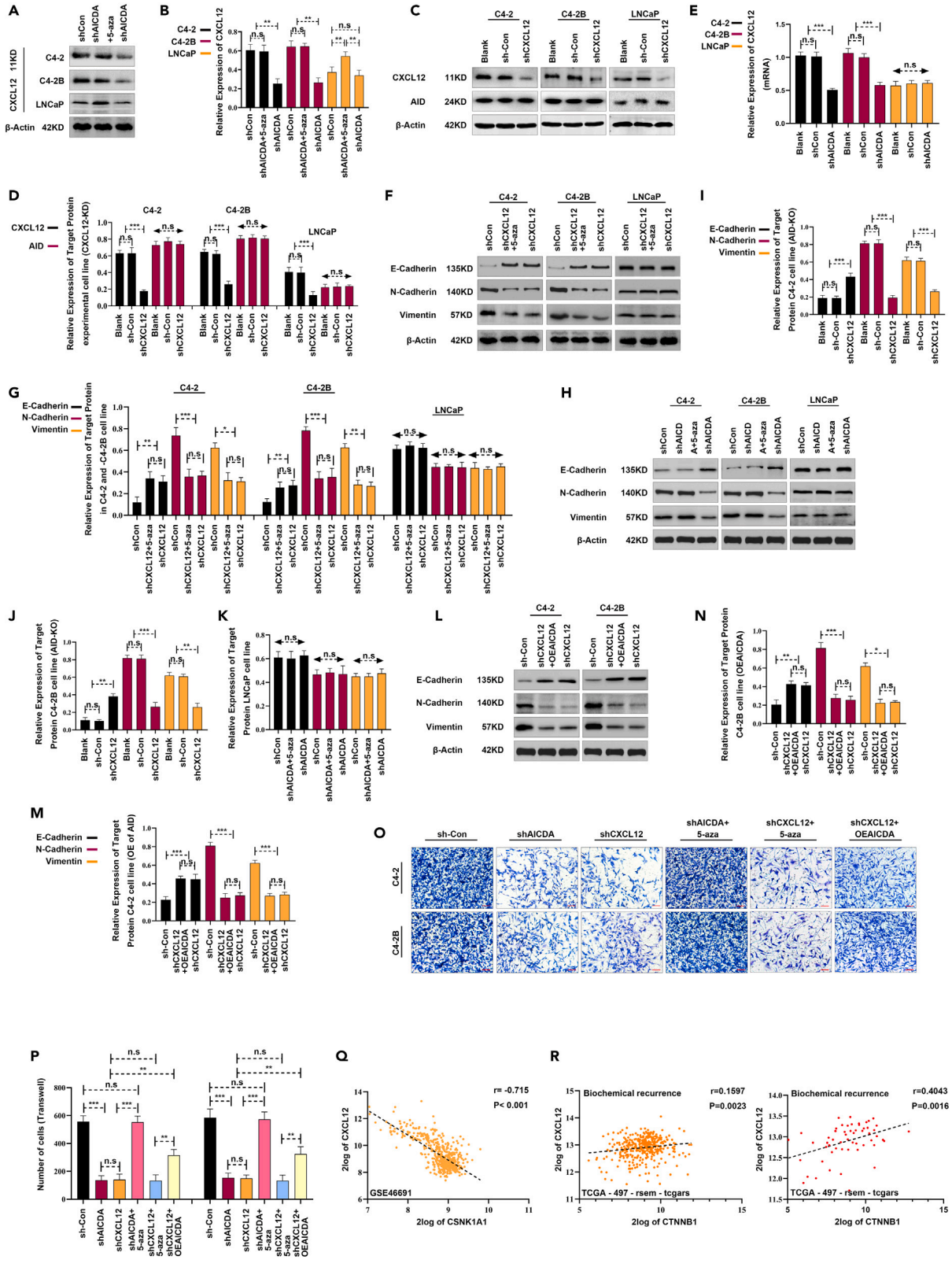
A
shCon
shAICDA
+5-aza
shAICDA
CXCL12 11KD
C4-2
C4-2B
LNCaP
β-Actin 42KD
B
C4-2
C4-2B
LNCaP
Relative Expression of CXCL12
shCon
shAICDA+5-aza
shAICDA
C
C4-2
C4-2B
LNCaP
Blank
sh-Con
shCXCL12
CXCL12 11KD
AID 24KD
β-Actin 42KD
E
C4-2
C4-2B
LNCaP
Relative Expression of CXCL12 (mRNA)
Blank
shCon
shAICDA
D
CXCL12
AID
C4-2
C4-2B
LNCaP
Relative Expression of Target Protein experimental cell line (CXCL12-KD)
Blank
sh-Con
shCXCL12
F
C4-2
C4-2B
LNCaP
shCon
shCXCL12 +5-aza
shCXCL12
E-Cadherin 135KD
N-Cadherin 140KD
Vimentin 57KD
β-Actin 42KD
I
E-Cadherin
N-Cadherin
Vimentin
Relative Expression of Target Protein C4-2 cell line (AID-KO)
Blank
sh-Con
shCXCL12
G
E-Cadherin
N-Cadherin
Vimentin
C4-2
C4-2B
LNCaP
Relative Expression of Target Protein in C4-2 and -C4-2B cell line
shCon
shCXCL12+5-aza
shCXCL12
H
C4-2
C4-2B
LNCaP
shCon
shAICD
A+5-aza
shAICDA
E-Cadherin 135KD
N-Cadherin 140KD
Vimentin 57KD
β-Actin 42KD
J
Relative Expression of Target Protein C4-2B cell line (AID-KO)
Blank
sh-Con
shCXCL12
K
Relative Expression of Target Protein LNCaP cell line
shCon
shAICDA+5-aza
shAICDA
L
C4-2
C4-2B
sh-Con
shCXCL12 +OEAICDA
shCXCL12
E-Cadherin 135KD
N-Cadherin 140KD
Vimentin 57KD
β-Actin 42KD
N
Relative Expression of Target Protein C4-2B cell line (OEAICDA)
sh-Con
shCXCL12 +OEAICDA
shCXCL12
M
E-Cadherin
N-Cadherin
Vimentin
Relative Expression of Target Protein C4-2 cell line (OE of AID)
sh-Con
shCXCL12 +OEAICDA
shCXCL12
O
sh-Con
shAICDA
shCXCL12
shAICDA+ 5-aza
shCXCL12+ 5-aza
shCXCL12+ OEAICDA
C4-2
C4-2B
P
Number of cells (Transwell)
sh-Con
shAICDA
shCXCL12
shAICDA+ 5-aza
shCXCL12+ 5-aza
shCXCL12+ OEAICDA
Q
r= -0.715
P< 0.001
GSE46691
2log of CXCL12
2log of CSNK1A1
R
Biochemical recurrence
r=0.1597
P=0.0023
TCGA - 497 - rsem - tcgars
2log of CXCL12
2log of CTNNB1
Biochemical recurrence
r=0.4043
P=0.0016
TCGA - 497 - rsem - tcgars
2log of CXCL12
2log of CTNNB1

Figure 4. AID promotes the EMT process in C4-2 and C4-2B cell lines through CXCL12 demethylation

(A and B) AID silencing significantly inhibited the expression of CXCL12 on protein level in C4-2 and C4-2B cells ($p < 0.01$), and there is no significant difference between shCon and shAICDA group in LNCaP cells ($p = 0.508$). The expression of CXCL12 in shAICDA+5-aza (50 nM, dissolved in PBS) group is remarkable than that in shAICDA group in C4-2 and C4-2B ($p < 0.01$) cells, and there is no significant difference between shCon and shAICDA+5-aza group ($p = 0.811$). Besides, the expression of CXCL12 in LNCaP cells was also upregulated by the demethylation reagent ($p < 0.01$). AICDA silencing-induced downregulation of CXCL12 was recovered by the treatment of 5-aza (50 nM, dissolved in PBS); furthermore, the expression of CXCL12 in LNCaP cells was also upregulated by the demethylation reagent.

(C and D) The shRNA-based specific sequence significantly inhibited the expression of CXCL12 in all experimental cell lines ($p < 0.001$); however, the expression of AID was not influenced by downregulation of CXCL12 ($p > 0.05$).

(E) RT-PCR demonstrated that the transcription of CXCL12 was remarkably suppressed by AICDA silencing in C4-2 and C4-2B cells ($p < 0.001$), and there is no significant difference between blank and shCon group ($p > 0.05$), and transcription of CXCL12 was not influenced by AICDA silencing in LNCaP cells ($p > 0.05$).

(F and G) CXCL12 silencing significantly downregulated the expression of N-cadherin and vimentin and upregulates the expression of E-cadherin in C4-2 ($p < 0.01$, <0.001 and <0.05) and C4-2B ($p < 0.001$) cells; however, the same result was not observed in LNCaP cells ($p > 0.05$). The treatment of 5-aza failed to recover the CXCL12 silencing-induced expression variation of E-cadherin, N-cadherin, and vimentin ($p > 0.05$).

(H–K) The treatment of 5-aza (50 nM, dissolved in PBS) converts the AICDA silencing-induced expression variation of E-cadherin, N-cadherin, and vimentin in C4-2 and C4-2B cells ($p < 0.001$), and as expected, there is no difference between shCon, shAICDA+5-aza, and shAICDA group ($p > 0.05$).

(L–N) The relative expression of EMT-related proteins including E-cadherin, N-cadherin, and vimentin was detected in shCon, shCXCL12 + OEAICDA, and shCXCL12 group, and OEAICDA failed to upregulate N-cadherin and vimentin, or downregulate E-cadherin in CXCL12-silenced C4-2 and C4-2B cells ($p > 0.05$).

(O and P) Transwell assay shows that both AICDA and CXCL12 silencing depressed the invasiveness of C4-2 ($p < 0.001$) and C4-2B ($p < 0.001$) cells, and 5-aza upregulates the invasiveness of AICDA-silenced C4-2 ($p < 0.001$ and <0.001) and C4-2B ($p < 0.001$ and <0.001) cells but CXCL12-silenced C4-2 and C4-2B cells ($p > 0.05$). Nevertheless, the invasiveness of CXCL12-silenced C4-2 and C4-2B cells was enhanced by overexpression of AICDA ($p < 0.01$), Scale bar, 50 μm.

(Q) The gene correlation analysis between CXCL12 and CSNK1A1 (encoding CK1α) based on database GSE46691. Pearson r values are used to indicate the level of correlation. The Pearson R value between CXCL12 and CSNK1A1 is −0.715 ($p < 0.001$).

(R) The gene correlation analysis between CXCL12 and CTNNB1 (encoding β-catenin) based on TCGA database (497 specimen). The R value is 0.1597 and 0.4043 in biochemical recurrence-free ($p = 0.0023$) and biochemical recurrence group ($p = 0.0016$), respectively. Two-sided Student's *t* test was used for A–P, Pearson correlation coefficient was used for Q and R. *$p < 0.05$, **$p < 0.01$, ***$p < 0.001$, n.s, no significance.

cell and however, the expression of EMT-related proteins, including CXCL12, E-cadherin, N-cadherin, and vimentin, was not affected; and overexpression of AICDA partially recover the CXCL12 silencing-induced invasiveness depression of C4-2 and C4-2B cells.

Besides, WLS was suppressed by AID knockdown (Figures 6A and 6B) and not influenced by CXCL12 silencing or 5-aza in C4-2, C4-2B, and LNCaP cells (Figures 6C–6E). In addition, AID overexpression enhanced the expression of WLS in all three cell lines (Figures 6C–6E). These results suggested that AID regulates WLS independent of CXCL12 in C4-2, C4-2B, and LNCaP cells. As the specific transporter of Wnt proteins, WLS is thought to assist in Wnt spreading between cells to activate the Wnt/β-catenin pathway and ultimately strengthen the EMT process. In our study, AID silencing downregulated WLS in all experimental cell lines. However, the expression of EMT-related proteins and invasion ability were quite different between CRPC and HSPC cells and we attribute these differences to the phosphorylation of β-catenin.

Subsequently, pyrvinium-treated C4-2 and C4-2B cells were used to study the impact of β-catenin on MMP14 expression. We found that the expression of MMP14 was suppressed by CK1α activator in C4-2 and C4-2B cells (Figures 6F and 6G). The results further confirmed that AID-CXCL12-β-catenin axis plays a role in the AID-induced upregulation of MMP14; however, it is not the only path in this regulatory relationship and more experiments are needed.

Transwell assay was performed to verify the results described previously. Consistently, the invasiveness of LNCaP was not inhibited by the pyrvinium and CXCL12 silencing, whereas the opposite result was observed in AICDA-silenced group, and 5-aza was unable to resist the AICDA silencing-induced invasiveness depression or upregulate the invasiveness of LNCaP cells in CXCL12-silenced group. Furthermore, overexpression of AID significantly enhanced the invasiveness of LNCaP cells (Figures 6H and 6I). These results demonstrated that CXCL12 is an outsider to the AID-induced upregulation of invasiveness in LNCaP cell line, and demethylation was not involved in the AID-related invasiveness enhancing of LNCaP cells.

Although the mechanism of how AID enhances the expression of MMP14 and WLS was not totally understood, the AID-induced upregulation of MMP14 and WLS was observed. The function of AID in promoting cancer progression has been demonstrated in various malignant diseases, including PCa. Thus, we consider that AID promotes the expression of MMP14 and WLS to facilitate the metastasis of PCa cells.

DISCUSSION

AID is a zinc-dependent DNA-editing enzyme located in chromosome 12q13, has high single-strand DNA-binding affinity, and drives gene expression profile. In past decade, quite a number of researches reported that AID is involved in various malignant diseases by inducing point mutation and demethylation, or participating in cancer-related inflammation. In our experiment, AICDA silencing-induced downregulation of N-cadherin and vimentin and upregulation of E-cadherin was recovered by the treatment of demethylation reagent 5-aza in C4-2 and C4-2B cells, whereas 5-aza was incapable to withstand CXCL12 silencing-induced expression variation of EMT-related proteins described previously; interestingly, AICDA silencing-induced CXCL12 depression was recovered by 5-aza; these results suggested that E-cadherin, N-cadherin, and Vimentin was not regulated by demethylation modification directly; furthermore, AID promoted CXCL12 expression through demethylation and further enhanced the EMT process in C4-2 and C4-2B cells by regulating those EMT-related proteins. Moreover, upregulation of CXCL12 inhibited the phosphorylation of β-catenin at S45 through the suppression of CK1α expression. Besides, AID facilitated the metastasis of PCa

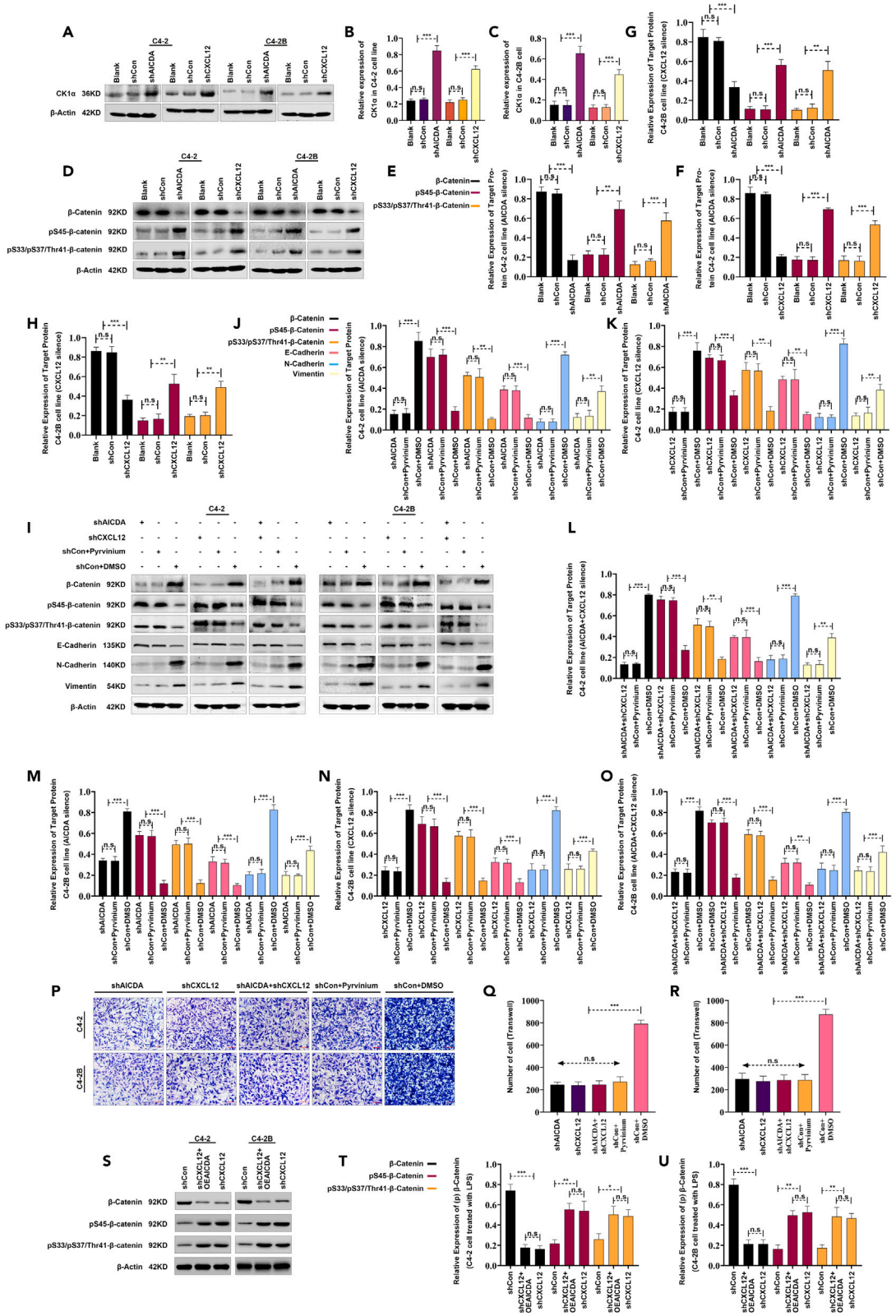
A
C4-2
C4-2B
Blank
shCon
shAICDA
shCXCL12
CK1α 36KD
β-Actin 42KD
B
Relative expression of CK1α in C4-2 cell line
C
Relative expression of CK1α in C4-2B cell
G
Relative Expression of Target Protein C4-2B cell line (CXCL12 silence)
D
β-Catenin 92KD
pS45-β-Catenin 92KD
pS33/pS37/Thr41-β-Catenin 92KD
β-Actin 42KD
E
β-Catenin
pS45-β-Catenin
pS33/pS37/Thr41-β-Catenin
Relative Expression of Target Protein C4-2 cell line (AICDA silence)
F
Relative Expression of Target Protein C4-2 cell line (AICDA silence)
H
Relative Expression of Target Protein C4-2B cell line (CXCL12 silence)
J
β-Catenin
pS45-β-Catenin
pS33/pS37/Thr41-β-Catenin
E-Cadherin
N-Cadherin
Vimentin
Relative Expression of Target Protein C4-2 cell line (AICDA silence)
K
Relative Expression of Target Protein C4-2 cell line (CXCL12 silence)
shAICDA
shCXCL12
shCon+Pyrvinium
shCon+DMSO
I
E-Cadherin 135KD
N-Cadherin 140KD
Vimentin 54KD
L
Relative Expression of Target Protein C4-2 cell line (AICDA+CXCL12 silence)
M
Relative Expression of Target Protein C4-2B cell line (AICDA silence)
N
Relative Expression of Target Protein C4-2B cell line (CXCL12 silence)
O
Relative Expression of Target Protein C4-2B cell line (AICDA+CXCL12 silence)
P
shAICDA
shCXCL12
shAICDA+shCXCL12
shCon+Pyrvinium
shCon+DMSO
C4-2
C4-2B
Q
Number of cell (Transwell)
R
Number of cell (Transwell)
S
shCXCL12+ OEAICDA
β-Catenin 92KD
pS45-β-catenin 92KD
pS33/pS37/Thr41-β-catenin 92KD
β-Actin 42KD
T
β-Catenin
pS45-β-Catenin
pS33/pS37/Thr41-β-Catenin
Relative Expression of (p) β-Catenin (C4-2 cell treated with LPS)
U
Relative Expression of (p) β-Catenin (C4-2B cell treated with LPS)

Figure 5. AID-induced upregulation of CXCL12 stabilizes β-catenin to enhance EMT by inhibiting CK1α in CRPC cells

(A–C) Expression of CK1α is significantly upregulated by both AICDA and CXCL12 silencing in C4-2 and C4-2B ($p < 0.001$) cells.

(D–H) AICDA and CXCL12 silencing significantly downregulates β-catenin and conversely promotes the expression of pS45-β-catenin and pS33/S37/Thr41-β-catenin in C4-2 (shAICDA: $p < 0.001$, <0.01 or <0.001; shCXCL12: $p < 0.001$) and C4-2B (shAICDA: $p < 0.0001$, <0.001, <0.01; shCXCL12: $p < 0.001$, <0.01 or <0.01) cell line.

(I–O) Pyrvinium significantly inhibits the expression of β-catenin ($p < 0.001$), N-cadherin ($p < 0.001$), and vimentin ($p < 0.01$, <0.001) and promotes the expression of pS45-β-catenin ($p < 0.001$), pS33/S37/Thr41-β-catenin ($p < 0.01$, <0.001), and E-cadherin in C4-2 and C4-2B cells ($p < 0.001$), and its inhibition efficiency was not statistical difference from shCon, shAICDA, shCXCL12, or shAICDA+shCXCL12 group ($p > 0.05$).

(P–R) Transwell assay shows that pyrvinium significantly suppresses the invasiveness of C4-2 and C4-2B cells ($p < 0.001$), and there is no significantly difference between shCon+ Pyrvinium and shAICDA and shCXCL12 or shAICDA+shCXCL12 group ($p > 0.05$). Scale bar, 50 μm.

(S–U) Overexpression of AID failed to upregulate β-catenin or downregulate pS45-β-catenin and pS33/S37/Thr41-β-Catenin in CXCL12 silenced C4-2 and C4-2B cells ($p > 0.05$). Student's *t* test or one-way ANOVA was used to evaluate statistical differences, and data are presented as the means ± standard deviation, every experiment is repeated three times. Two-sided Student's *t* test was used for all panels. *$p < 0.05$, **$p < 0.01$, ***$p < 0.001$, n.s, no significance.

cells by enhancing the expression of MMP14 through the demethylation of CXCL12 partly. Although 5-aza failed to regulate the target proteins expression in LNCaP cells, AICDA silencing-caused suppression of MMP14 and WLS was observed; these results indicated that AID not only promotes the EMT process of CRPC cell line by regulated CXCL12 through demethylation, but also facilitates the metastasis of PCa cell line by enhanced extracellular matrix degradation and Wnts transportation. However, the gene-specific targeting of AID is not fully understood, and the mechanism of upregulation of MMP14 and WLS by AID through non-demethylation approach remains unclear, and further research is needed.

Since the discovery of Honjo, much effort has been carried out to determine the mechanism of the chaotic biological progress caused by AID. The main molecular structural character of AID is catalytic domain with typical α-β-α Zn^{2+} binding modification, which consists HXEX (23–28) PCX (2–4) C (X is any amino acid) and thus provides one histidine and two cysteines as Zn^{2+}-coordinating residues to collaborate with glutamic acid and deaminize dC through nucleophilic attack.[29] According to the inferior catalytic efficiency of AID than that of a typical enzyme, multiple approaches were used to explore the regulation of AID activation. The most fascinating approach is the conformational dynamics theory. King et al. identified several secondary catalytic loops that comprise the 21 non-constituent amino acids of AID that regulate the accessibility of catalytic pocket by fluid dynamics to determine catalytic efficiency.[30] Therein, loop 2 (L2, comprises G23, R24, R25, E26, T27, and L29 residues) and loop 8 (L8, comprises Y114, F115, and E122 residues) are considered to mediate 5-mC tolerance, substrate specificity, and dC stabilization.[31] Hence, L2 and L8 are the potential managers of AID-induced demethylation.

Besides, Bachl et al. demonstrated that immunoglobulin (Ig) gene transcriptional activation is based on specific enhancer; κ intron and κ3′ enhancer is associated with hypermutation rate.[32] This observation indicated that enhancer is a potential guide for AID-induced deamination, as well as AID-induced demethylation, theoretically.

Indeed, existing evidence revealed that transcription activation is insufficient to induce AID target genes unless the genes coexist with the activated enhancers. Certain histones in chromatin, such as H3K27Ac and H3K4me1, are substantial markers of enhancer activation. TC-seq-based exploration demonstrated that AID hotspot region highly overlaps with H3K27Ac and H3K4me1 modification.[33] Moreover, transcription factors, such as E2A and PAX5, drive the distribution of AID in the genome by binding at the enhancers of Ig gene.[34]

Ten-eleven translocation (TET) proteins, including TET1/2/3, are a collection of dioxygenases that induce the Fe^{2+} and α-ketoglutarate-dependent iterative oxidation of 5-hydroxymethylcytosine (5hmC) → 5-formylcytosine (5fC) → 5-carboxylcytosine (5caC) conversion.[35] Similar with AID-induced demethylation, 5fC and 5caC are recognized by TDG and followed up with BER activation to realize demethylation.[36] The physical processivity of TET is analogous to slide along the DNA from one CpG island to another, whereas TET, which induced 5mC-to-5caC conversion, is iteratively catalyzed without releasing substrates in chemical processivity.[36] We speculated that similar with competitive inhibition, CpG islands located downstream of initial binding site are occupied by other TETs and result in chemical processivity. On the contrary, physical processivity is activated under TET deficiency. Biochemical, structure and enzyme dynamics studies revealed that TETs prefer 5mC rather than 5hmC or 5fC, and the discrepant ability of all three substrates in hydrogen attraction led to the preferential catalysis of 5mC by TET2.[37] Furthermore, the mutation of specific amino acid residues (mainly in catalyze domain) in TET2 causes a similar selection bias of substrate as described previously.[35] According to a previous study, TETs are involved in PCa. Shivani Kamdar et al. showed that TET2 was suppressed in androgen-sensitive PCa and drives several PCa-related genes expression through methylation modification.[38] Additionally, hypoxic intracellular environment and TET gene mutation in androgen-dependent PCa are capable of downregulating the capacity of TETs to catalyze.[39] These previous studies indicated that TET-induced demethylation is deprived in androgen-sensitive PCa. However, based on the mechanism described previously, TETs would like to be released from androgen-induced suppression. The distribution of TET-induced 5hmC highly overlaps with the enhancer activation markers H3K27Ac and H3K4me1. Moreover, TETs participate in the activation of the enhancer by collaborating with transcription factors, such as C/EBPa, Klf4, and Tfcp2l1, to increase chromatin accessibility and facilitate biological progress, such as transcription initiation.[40] Interestingly, Chan-Wang et al. identified that transcription factor E2A recruits TETs to activate the enhancer.[41] Similarly, AID is also driven by E2A and attracted by the opening of the chromosomal frame as mentioned previously. Furthermore, Jiao and colleagues reported that AID collaborates with TET2 to induce the demethylation of FANCA promoter in diffuse large B cell lymphoma and confirmed the protein-protein interaction between two demethylation drivers through immunoprecipitation assay.[42] Based on the mechanism described previously, we hypothesis that E2A recruits ectopic TETs to trigger the activation of CXCL12 enhancer through the catalytic oxidation of 5mC. Subsequently AID is tempted by H3K27Ac and H3K4me1 to recognize the target gene to realizing TET-based demethylation in CRPC cells.

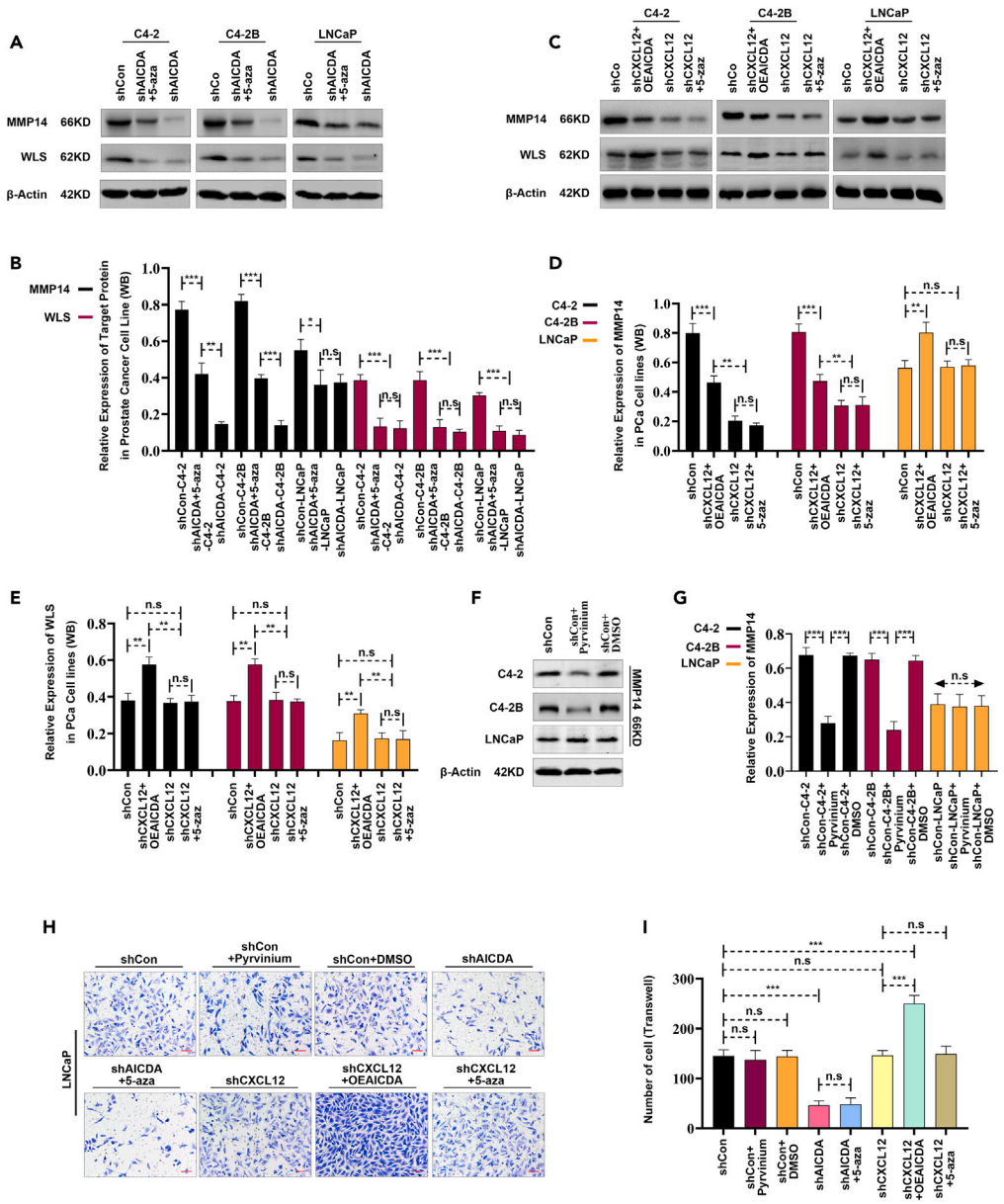

Figure 6. AID facilitates the metastasis of PCa cells by upregulating MMP14 and WLS

(A and B) AICDA silencing significantly downregulates the expression of MMP14 and WLS in C4-2 ($p < 0.001$), C4-2B ($p < 0.001$), and LNCaP ($p < 0.05$, <0.001) cells. 5-Aza partially rescued AICDA silencing caused by MMP14 depression in C4-2 ($p < 0.01$) and C4-2B ($p < 0.001$) cells, and expression of WLS was not influenced by 5-aza significantly in all experimental cell lines ($p > 0.05$).

(C–E) CXCL12 silencing obviously inhibits the expression of MMP14 in C4-2 ($p < 0.001$) and C4-2B cells ($p < 0.001$) but not in LNCaP cells ($p > 0.05$), and the expression of WLS was not influenced by CXCL12 silencing significantly in all experimental cell lines ($p > 0.05$) and overexpression of AICDA dramatically upregulated the expression of WLS in all three experimental cell lines ($p < 0.01$). 5-Aza was unable to upregulate the expression of MMP14 and WLS in CXCL12-silenced experimental cell lines ($p > 0.05$), and overexpression of AICDA partially recover or promote the expression level of MMP14 in CXCL12-silenced C4-2 and C4-2B cells ($p < 0.01$) or LNCaP ($p < 0.01$) cells, respectively.

(F and G) CK1α-specific activator pyrvinium remarkably downregulated the expression of MMP14 in C4-2 ($p < 0.001$) and C4-2B ($p < 0.001$) cells, whereas is unfunctional in upregulated MMP14 in LNCaP cells ($p > 0.05$).

(H and I) Transwell assay showed that AICDA silencing suppressed the invasiveness of LNCaP obviously ($p < 0.001$), there is no difference of invasiveness between shCon group and pyrvinium, CXCL12 knockdown, 5-aza group ($p > 0.05$), and overexpression of AICDA dramatically enhanced the invasiveness of LNCaP cells ($p < 0.001$), Scale bar, 50 μm. Two-sided Student's *t* test was used for all panels. *$p < 0.05$, **$p < 0.01$, ***$p < 0.001$, n.s, no significance.

The knowledge-based inclusion criteria were used to further explore the mechanism of CRPC metastasis caused by AID-induced demethylation. A set of factors, including CXCL12, E-cadherin, N-cadherin, vimentin, β-catenin, MMP14, and WLS, were detected in the protein level under different conditions. In our study, the upregulation of CXCL12 caused by AID-induced demethylation enhanced the expression of β-catenin, and the upregulation of EMT-related proteins, such as N-cadherin and vimentin, indicated that AID promotes the EMT process in CRPC by the demethylation of CXCL12. CK1α is encoded by CSNK1A1, which contains four splicing transcript variants and is distinguished by the insertion of amino acid segment "L" or "S."[43] A previous study showed that CK1α is involved in the phosphorylation of certain proteins to regulate various biological processes, such as the inhibition of the activation of the Wnt/β-catenin pathway. CK1α-produced pS45-β-catenin is required for GSK3β-induced pS33/S37/T41-β-catenin phosphorylation and plays a crucial in the ubiquitination and degradation of β-catenin.[44] Nevertheless, the regulation of CK1α is not fully understood.

Budini et al. reported that the last four serine and threonine residues located in the carboxyl terminal of CK1α undergo autophosphorylation and result in the inhibition of catalytic activity.[45] Crystal structure analysis showed that β-hairpin loop and CRL4CRBN E3 ubiquitin ligase participate in the ubiquitination of CK1α and facilitate proteasome-based degradation.[46,47] Moreover, glioma pathogenesis-related protein 1 and murine double minute X are reported to regulate translocation kinase activity, respectively.[48,49] Besides, Dimova et al. revealed that SDF-1 mediates the downregulation of CK1α in cardiac stem/progenitor cells.[50] Unfortunately, how the AID-induced upregulation of CXCL12 inhibits the expression of CK1α remains unclear and needs further exploration.

In conclusion, AID upregulates CXCL12 by demethylation and, subsequently, reinforces the stability of β-catenin through the CXCL12-induced inhibition of CK1α and finally enhances EMT in CRPC cells. In addition, the AID-induced upregulation of MMP14 and WLS contributes to the degradation of the extracellular matrix and the induction of the Wnt/β-catenin pathway to promote the metastasis of PCa, respectively. Although the mechanism of the AID-induced demethylation and inhibition of CK1α is not entirely clear, the expected results are observed in our experiment and these results suggest that AID is a potential therapeutic target of PCa.

Limitations of the study

Although our work demonstrated that AID promotes the metastasis of CRPC through demethylation, AID-induced methylation heterogeneity of CXCL12 promoter was not observed directly, and bisulfite sequencing should be performed in the following study. Moreover, the underlying mechanism of AID selection of demethylation sites in PCa remains unclear, and multiple sequencing methods should be performed in the further study.

STAR★METHODS

Detailed methods are provided in the online version of this paper and include the following:

- KEY RESOURCES TABLE
- RESOURCE AVAILABILITY
  - Lead contact
  - Materials availability
  - Data and code availability
- EXPERIMENT MODEL AND STUDY PARTICIPANT DETAILS
  - Cell line and cell culture
  - Patient selection and tissue preparation
  - Mice
- METHOD DETAILS
  - Transfection
  - Western blot assay
  - Immunohistochemistry
  - Immunofluorescence staining
  - Real-time fluorescent quantitative PCR
  - Transwell
  - CCK-8 assay
  - Animal experiment
- QUANTIFICATION AND STATISTICAL ANALYSIS

SUPPLEMENTAL INFORMATION

Supplemental information can be found online at https://doi.org/10.1016/j.isci.2023.108523.

ACKNOWLEDGMENTS

This work was supported by the National Natural Science Foundation of China (82372966) and the Key Research and Development Program of Hainan Province (2019122 and 2020136).

AUTHOR CONTRIBUTIONS

Q.L. took part in the majority of experiments and writing articles. J.F. took part in the majority of experiments. Z.Z. screened out the AID and CXCL12-specific sequence with the best suppression rate and provided software application support. Z.M. took part in the BSP assay and subsequently analysis. Y.J. took part in the WB, IHC, and IF assay. Y.W. participated in the cell culture experimental design. X.Y. took part in the experimental design and transwell assay. P.L. designed the experiments and took part in the transfection. H.L. designed the experiments and helped write the manuscript, participated in the establishment of nude mice mode and gene correlation analysis, and also is the manager of this research.

DECLARATION OF INTERESTS

The authors declare no conflict of interest.

INCLUSION AND DIVERSITY

We support inclusive, diverse, and equitable conduct of research.

Received: April 10, 2023
Revised: November 14, 2023
Accepted: November 20, 2023
Published: November 23, 2023

REFERENCES

1. Sung, H., Ferlay, J., Siegel, R.L., Laversanne, M., Soerjomataram, I., Jemal, A., and Bray, F. (2021). Global Cancer Statistics 2020: GLOBOCAN Estimates of Incidence and Mortality Worldwide for 36 Cancers in 185 Countries. CA. Cancer J. Clin. *71*, 209–249.
2. Deshmukh, A., Arfuso, F., Newsholme, P., and Dharmarajan, A. (2019). Epigenetic demethylation of sFRPs, with emphasis on sFRP4 activation, leading to Wnt signalling suppression and histone modifications in breast, prostate, and ovary cancer stem cells. Int. J. Biochem. Cell Biol. *109*, 23–32.
3. Dominguez, P.M., and Shaknovich, R. (2014). Epigenetic function of activation-induced cytidine deaminase and its link to lymphomagenesis. Front. Immunol. *5*, 642.
4. Nishida, J., Momoi, Y., Miyakuni, K., Tamura, Y., Takahashi, K., Koinuma, D., Miyazono, K., and Ehata, S. (2020). Epigenetic remodelling shapes inflammatory renal cancer and neutrophil-dependent metastasis. Nat. Cell Biol. *22*, 465–475.
5. Jiang, Z., Zhang, Y., Chen, X., Wu, P., and Chen, D. (2020). Long non-coding RNA LINC00673 silencing inhibits proliferation and drug resistance of prostate cancer cells via decreasing KLF4 promoter methylation. J. Cell Mol. Med. *24*, 1878–1892.
6. Li, N., Dhar, S.S., Chen, T.Y., Kan, P.Y., Wei, Y., Kim, J.H., Chan, C.H., Lin, H.K., Hung, M.C., and Lee, M.G. (2016). JARID1D Is a Suppressor and Prognostic Marker of Prostate Cancer Invasion and Metastasis. Cancer Res. *76*, 831–843.
7. Feng, Y., Seija, N., Di Noia, J.M., and Martin, A. (2020). AID in Antibody Diversification: There and Back Again. Trends Immunol. *41*, 586–600.
8. Li, H., Li, Q., Ma, Z., Zhou, Z., Fan, J., Jin, Y., Wu, Y., Cheng, F., and Liang, P. (2019). AID modulates carcinogenesis network via DNA demethylation in bladder urothelial cell carcinoma. Cell Death Dis. *10*, 251.
9. Teater, M., Dominguez, P.M., Redmond, D., Chen, Z., Ennishi, D., Scott, D.W., Cimmino, L., Ghione, P., Chaudhuri, J., Gascoyne, R.D., et al. (2018). AICDA drives epigenetic heterogeneity and accelerates germinal center-derived lymphomagenesis. Nat. Commun. *9*, 222.
10. Eso, Y., Takai, A., Matsumoto, T., Inuzuka, T., Horie, T., Ono, K., Uemoto, S., Lee, K., Edelmann, W., Chiba, T., and Marusawa, H. (2016). MSH2 Dysregulation Is Triggered by Proinflammatory Cytokine Stimulation and Is Associated with Liver Cancer Development. Cancer Res. *76*, 4383–4393.
11. Ramiro, A.R., and Barreto, V.M. (2015). Activation-induced cytidine deaminase and active DNA demethylation. Trends Biochem. Sci. *40*, 172–181.
12. Shimizu, T., Marusawa, H., Endo, Y., and Chiba, T. (2012). Inflammation-mediated genomic instability: roles of activation-induced cytidine deaminase in carcinogenesis. Cancer Sci. *103*, 1201–1206.
13. Tong, D., Liu, Q., Liu, G., Xu, J., Lan, W., Jiang, Y., Xiao, H., Zhang, D., and Jiang, J. (2017). Metformin inhibits castration-induced EMT in prostate cancer by repressing COX2/PGE2/STAT3 axis. Cancer Lett. *389*, 23–32.
14. Han, I.H., Kim, J.H., Jang, K.S., and Ryu, J.S. (2019). Inflammatory mediators of prostate epithelial cells stimulated with Trichomonas vaginalis promote proliferative and invasive properties of prostate cancer cells. Prostate *79*, 1133–1146.
15. Lee, H., Trott, J.S., Haque, S., McCormick, S., Chiorazzi, N., and Mongini, P.K.A. (2010). A cyclooxygenase-2/prostaglandin E2 pathway augments activation-induced cytosine deaminase expression within replicating human B cells. J. Immunol. *185*, 5300–5314.
16. Janssens, R., Struyf, S., and Proost, P. (2018). The unique structural and functional features of CXCL12. Cell. Mol. Immunol. *15*, 299–311.
17. Tolić, A., Grdović, N., Dinić, S., Rajić, J., Đorđević, M., Sinadinović, M., Arambašić Jovanović, J., Mihailović, M., Poznanović, G., Uskoković, A., and Vidaković, M. (2019). Absence of PARP-1 affects Cxcl12 expression by increasing DNA demethylation. J. Cell Mol. Med. *23*, 2610–2618.
18. Morein, D., Erlichman, N., and Ben-Baruch, A. (2020). Beyond Cell Motility: The Expanding Roles of Chemokines and Their Receptors in Malignancy. Front. Immunol. *11*, 952.
19. Guo, F., Wang, Y., Liu, J., Mok, S.C., Xue, F., and Zhang, W. (2016). CXCL12/CXCR4: a symbiotic bridge linking cancer cells and their stromal neighbors in oncogenic communication networks. Oncogene *35*, 816–826.
20. Port, F., and Basler, K. (2010). Wnt trafficking: new insights into Wnt maturation, secretion and spreading. Traffic *11*, 1265–1271.
21. Chiou, S.S., Wang, L.T., Huang, S.B., Chai, C.Y., Wang, S.N., Liao, Y.M., Lin, P.C., Liu, K.Y., and Hsu, S.H. (2014). Wntless (GPR177) expression correlates with poor prognosis in B-cell precursor acute lymphoblastic leukemia via Wnt signaling. Carcinogenesis *35*, 2357–2364.
22. Augustin, I., Dewi, D.L., Hundshammer, J., Erdmann, G., Kerr, G., and Boutros, M. (2017). Wnt regulates the survival and genomic stability of embryonic stem cells. Sci. Signal. *10*, eaah6829.
23. Bugter, J.M., Fenderico, N., and Maurice, M.M. (2021). Mutations and mechanisms of WNT pathway tumour suppressors in cancer. Nat. Rev. Cancer *21*, 5–21.
24. Nusse, R., and Clevers, H. (2017). Wnt/beta-Catenin Signaling, Disease, and Emerging Therapeutic Modalities. Cell *169*, 985–999.
25. Valenta, T., Hausmann, G., and Basler, K. (2012). The many faces and functions of beta-catenin. EMBO J. *31*, 2714–2736.
26. Pal, I., Rajesh, Y., Banik, P., Dey, G., Dey, K.K., Bharti, R., Naskar, D., Chakraborty, S., Ghosh, S.K., Das, S.K., et al. (2019). Prevention of epithelial to mesenchymal transition in colorectal carcinoma by regulation of the E-cadherin-beta-catenin-vinculin axis. Cancer Lett. *452*, 254–263.
27. Prasad, R., and Katiyar, S.K. (2014). Ultraviolet radiation-induced inflammation activates beta-catenin signaling in mouse skin and skin tumors. Int. J. Oncol. *44*, 1199–1206.
28. Akcora, B.Ö., Storm, G., and Bansal, R. (2018). Inhibition of canonical WNT signaling pathway by beta-catenin/CBP inhibitor ICG-001 ameliorates liver fibrosis *in vivo* through

suppression of stromal CXCL12. Biochim. Biophys. Acta, Mol. Basis Dis. *1864*, 804–818.
29. Barreto, V.M., and Magor, B.G. (2011). Activation-induced cytidine deaminase structure and functions: a species comparative view. Dev. Comp. Immunol. *35*, 991–1007.
30. King, J.J., Manuel, C.A., Barrett, C.V., Raber, S., Lucas, H., Sutter, P., and Larijani, M. (2015). Catalytic pocket inaccessibility of activation-induced cytidine deaminase is a safeguard against excessive mutagenic activity. Structure *23*, 615–627.
31. King, J.J., and Larijani, M. (2017). A Novel Regulator of Activation-Induced Cytidine Deaminase/APOBECs in Immunity and Cancer: Schrodinger's CATalytic Pocket. Front. Immunol. *8*, 351.
32. Bachl, J., Olsson, C., Chitkara, N., and Wabl, M. (1998). The Ig mutator is dependent on the presence, position, and orientation of the large intron enhancer. Proc. Natl. Acad. Sci. USA *95*, 2396–2399.
33. Wang, Q., Oliveira, T., Jankovic, M., Silva, I.T., Hakim, O., Yao, K., Gazumyan, A., Mayer, C.T., Pavri, R., Casellas, R., et al. (2014). Epigenetic targeting of activation-induced cytidine deaminase. Proc. Natl. Acad. Sci. USA *111*, 18667–18672.
34. Grundström, C., Kumar, A., Priya, A., Negi, N., and Grundström, T. (2018). ETS1 and PAX5 transcription factors recruit AID to Igh DNA. Eur. J. Immunol. *48*, 1687–1697.
35. Scourzic, L., Mouly, E., and Bernard, O.A. (2015). TET proteins and the control of cytosine demethylation in cancer. Genome Med. *7*, 9.
36. Wu, X., and Zhang, Y. (2017). TET-mediated active DNA demethylation: mechanism, function and beyond. Nat. Rev. Genet. *18*, 517–534.
37. Hu, L., Lu, J., Cheng, J., Rao, Q., Li, Z., Hou, H., Lou, Z., Zhang, L., Li, W., Gong, W., et al. (2015). Structural insight into substrate preference for TET-mediated oxidation. Nature *527*, 118–122.
38. Kamdar, S., Isserlin, R., Van der Kwast, T., Zlotta, A.R., Bader, G.D., Fleshner, N.E., and Bapat, B. (2019). Exploring targets of TET2-mediated methylation reprogramming as potential discriminators of prostate cancer progression. Clin. Epigenet. *11*, 54.
39. Smeets, E., Lynch, A.G., Prekovic, S., Van den Broeck, T., Moris, L., Helsen, C., Joniau, S., Claessens, F., and Massie, C.E. (2018). The role of TET-mediated DNA hydroxymethylation in prostate cancer. Mol. Cell. Endocrinol. *462*, 41–55.
40. Sardina, J.L., Collombet, S., Tian, T.V., Gómez, A., Di Stefano, B., Berenguer, C., Brumbaugh, J., Stadhouders, R., Segura-Morales, C., Gut, M., et al. (2018). Transcription Factors Drive Tet2-Mediated Enhancer Demethylation to Reprogram Cell Fate. Cell Stem Cell *23*, 727–741.e9.
41. Lio, C.W., Zhang, J., González-Avalos, E., Hogan, P.G., Chang, X., and Rao, A. (2016). Tet2 and Tet3 cooperate with B-lineage transcription factors to regulate DNA modification and chromatin accessibility. Elife *5*, e18290.
42. Jiao, J., Jin, Y., Zheng, M., Zhang, H., Yuan, M., Lv, Z., Odhiambo, W., Yu, X., Zhang, P., Li, C., et al. (2019). AID and TET2 co-operation modulates FANCA expression by active demethylation in diffuse large B cell lymphoma. Clin. Exp. Immunol. *195*, 190–201.
43. Jiang, S., Zhang, M., Sun, J., and Yang, X. (2018). Casein kinase 1alpha: biological mechanisms and theranostic potential. Cell Commun. Signal. *16*, 23.
44. Shen, C., Nayak, A., Melendez, R.A., Wynn, D.T., Jackson, J., Lee, E., Ahmed, Y., and Robbins, D.J. (2020). Casein Kinase 1α as a Regulator of Wnt-Driven Cancer. Int. J. Mol. Sci. *21*, 5940.
45. Budini, M., Jacob, G., Jedlicki, A., Pérez, C., Allende, C.C., and Allende, J.E. (2009). Autophosphorylation of carboxy-terminal residues inhibits the activity of protein kinase CK1alpha. J. Cell. Biochem. *106*, 399–408.
46. Krönke, J., Fink, E.C., Hollenbach, P.W., MacBeth, K.J., Hurst, S.N., Udeshi, N.D., Chamberlain, P.P., Mani, D.R., Man, H.W., Gandhi, A.K., et al. (2015). Lenalidomide induces ubiquitination and degradation of CK1alpha in del(5q) MDS. Nature *523*, 183–188.
47. Petzold, G., Fischer, E.S., and Thomä, N.H. (2016). Structural basis of lenalidomide-induced CK1alpha degradation by the CRL4(CRBN) ubiquitin ligase. Nature *532*, 127–130.
48. Li, L., Ren, C., Yang, G., Fattah, E.A., Goltsov, A.A., Kim, S.M., Lee, J.-S., Park, S., Demayo, F.J., Ittmann, M.M., et al. (2011). GLIPR1 Suppresses Prostate Cancer Development through Targeted Oncoprotein Destruction. Cancer Res. *71*, 7694–7704.
49. Ueda, K., Kumari, R., Schwenger, E., Wheat, J.C., Bohorquez, O., Narayanagari, S.-R., Taylor, S.J., Carvajal, L.A., Pradhan, K., Bartholdy, B., et al. (2021). MDMX acts as a pervasive preleukemic-to-acute myeloid leukemia transition mechanism. Cancer Cell *39*, 529–547.e7.
50. Dimova, N., Wysoczynski, M., and Rokosh, G. (2014). Stromal cell derived factor-1alpha promotes C-Kit+ cardiac stem/progenitor cell quiescence through casein kinase 1alpha and GSK3beta. Stem Cell. *32*, 487–499.

STAR★METHODS

KEY RESOURCES TABLE

REAGENT or RESOURCE	SOURCE	IDENTIFIER
Antibodies		
Mouse monoclonal anti-AID	Cell Signaling Technology	Cat# 4959; RRID: AB_10692771
Rabbit polyclonal anti-AID	Abcam	Cat# ab93596; RRID: AB_10565035)
Mouse monoclonal anti-E-Cadherin	Cell Signaling Technology	Cat# 14472; RRID: AB_2728770)
Rabbit polyclonal anti-CXCL12	Abcam	Cat# ab9797; RRID: AB_296627
Rabbit monoclonal anti-N-Cadherin	Cell Signaling Technology	Cat# 13116; RRID: AB_2687616
Rabbit monoclonal anti-Vimentin	Cell Signaling Technology	Cat# 5741; RRID: AB_10695459
Rabbit monoclonal anti-MMP14	Abcam	Cat# ab51074; RRID: AB_881234
Chicken polyclonal anti-WLS	Abcam	Cat# ab72385; RRID: AB_1269023
Rabbit polyclonal anti-WLS	Thermo Fisher Scientific	Cat# PA5-98483; RRID: AB_2813096
Rabbit monoclonal anti-β-Catenin	Cell Signaling Technology	Cat# 8480; RRID: AB_11127855
Rabbit polyclonal anti-pS45-β-Catenin	Cell Signaling Technology	Cat# 9564; RRID: AB_331150
Rabbit monoclonal anti-pS33/ pS37/Thr41-β-Catenin	Cell Signaling Technology	Cat# 9561; RRID: AB_331729
Mouse monoclonal anti-β-Actin	Abcam	Cat# ab8226; RRID: AB_306371
Bacterial and virus strains		
E. Coli strain DH5α	TIANGEN	CB101-02
Biological samples		
Human prostate cancer tissue	Renmin Hospital of Wuhan University	N/A
Human prostatic hyperplasia with chronic prostatitis tissue	Renmin Hospital of Wuhan University	N/A
Human normal prostate tissue	Renmin Hospital of Wuhan University	N/A
Chemicals, peptides, and recombinant proteins		
Pyrvinium	Sigma-Aldrich	Cat#P0027
DMSO	Sigma-Aldrich	Cat#D2650
Trichloromethane	Sinopharm Chemical Reagent	Cat#10006818
Isopropanol	Sinopharm Chemical Reagent	Cat#80109218
Absolute ethyl alcohol	Sinopharm Chemical Reagent	Cat#10009218
GeneRuler 1 kb DNA Ladder	Thermo Scientific	Cat #SM0311
NormalRunTM 250bp-II DNA Ladder	GeneRay	Cat #DL2502
PrimeSTAR HS DNA polymerase	Takara	Cat #R010B
Taq Plus DNA polymerase	Vazyme	Cat #P201-D3
T4 DNA ligase	Thermo Scientific	Cat #EL0016
Critical commercial assays		
PureLink™ Genomic DNA Mini Kit	Thermo Fisher Scientific	Cat#K182002
AceQ Universal SYBR qPCR Master Mix	Vazyme biotech	Cat#Q511-02
TRIpure Reagent	Aidlab Biotechnologies	Cat#RN01
Revertaid reverse transcriptase	Thermo Fisher Scientific	Cat#EP0442
EndoFree midi Plasmid Kit	TIANGEN	Cat #DP118-2
ClonExpressTM II One Step Cloning Kit	Vazyme	Cat #C122
Cell Counting Kit-8	MedChemExpress	Cat #HY-K0301

(*Continued on next page*)

Continued

REAGENT or RESOURCE	SOURCE	IDENTIFIER
dNTPmix	Thermo Fisher Scientific	Cat#R0191
RiboLock RNase	Thermo Fisher Scientific	Cat#EO0384
Deposited data		
Raw and analyzed data	GEO	https://www.ncbi.nlm.nih.gov/geo/query/acc.cgi?acc=GSE21034
Raw and analyzed data	GEO	https://www.ncbi.nlm.nih.gov/geo/query/acc.cgi?acc=GSE46691
Raw and analyzed data	TCGA	https://hgserver1.amc.nl/cgibin/r2/main.cgi
Raw and analyzed data	GEO	https://www.ncbi.nlm.nih.gov/geo/query/acc.cgi?acc=GSE97284
Raw and analyzed data	GEO	https://www.ncbi.nlm.nih.gov/geo/query/acc.cgi?acc=GSE70769
Experimental models: Cell lines		
Human C4-2	ATCC	Cat#CRL-3314
Human C4-2B	ATCC	Cat#CRL-3315
Human LNCaP	Procell	Cat#CL-0143
Human 22RV1	Procell	Cat#CL-0004
Human DU145	ATCC	Cat#HTB-81
Human PC3	Procell	Cat#CL-0185
Experimental models: Organisms/strains		
BLAB/c Nude mice	Charles River Laboratory	Cat# 490 (Homozygous)
Oligonucleotides		
hActin-F-primer: GTCCACCGCAAATGCTTCTA CACCGTTC	This paper	N/A
hActin-R-primer:TGCTGTCACCTT	This paper	N/A
hCXCL12-F-primer:GCTACAGATGCCCATGCCGAT	This paper	N/A
hCXCL12-R-primer:AGCTTCGGGTCAATGCACACT	This paper	N/A
Target gene fragment acquisition-AICDA-F-primer	GAGGATCCCCGGGTACCGGTCG CCACC ATGGCGGAGCCGAGCGGC	N/A
Target gene fragment acquisition-AICDA-R-primer	TCACCATGGTGGCGACCGGGCTG ACACTCAACTGAGCA	N/A
Target gene identification primer-AICDA-F-primer	CCACCCAATGCTAATGAAG	N/A
Target gene identification primer-AICDA-R-primer	CGTCGCCGTCCAGCTCGACCAG	N/A
shRNA-AICDA #1: TGACTTACGAGACGCATTT	This paper	N/A
shRNA-AICDA #2: TTTCGTACTTTGGGACTTT	This paper	N/A
shRNA-CXCL12 #1: TGTGCATTGACCCGAAGCTAA	This paper	N/A
shRNA-CXCL12 #2: GCCAACGTCAAGCATCTCAAA	This paper	N/A
Recombinant DNA		
hU6-MCS-Ubiquitin-EGFP-IRES-puromycin	This paper	N/A
Ubi-MCS-3FLAG-CBh-gcGFP-IRES-puromycin	This paper	N/A
Software and algorithms		
SPSS Statistics version 19.0	IBM	https://www.ibm.com/cn-zh/products/spss-statistics
Graph-Pad Prism 8 version 9.0.0 software	GraphPad	https://www.graphpad.com/features

(*Continued on next page*)

Continued

REAGENT or RESOURCE	SOURCE	IDENTIFIER
R software (4.1.2)	R	https://cran.r-project.org/bin/windows/base/old/4.1.2/
Image J 1.52v	ImageJ	https://imagej.net/ij/
Figdraw	Home for Researchers	https://www.figdraw.com/#/

RESOURCE AVAILABILITY

Lead contact

Requests for further information should be directed to and will be fulfilled by the lead contact, Haoyong Li (RM002243@whu.edu.cn).

Materials availability

This study did not generate new unique reagents.

Data and code availability

- This paper analyzes existing, publicly available data. These accession numbers for the datasets are listed in the key resources table.
- This paper does not report original code.
- Any additional information required to reanalyze the data reported in this paper is available from the lead contact upon reasonable request.

EXPERIMENT MODEL AND STUDY PARTICIPANT DETAILS

Cell line and cell culture

Experimental cell lines including LNCaP, PC-3 and 22RV1 were purchased from Procell Biotechnology Limited Corporation (Wuhan, China), and C4-2, C4-2B and DU145 were purchased from American Type Culture Collection (ATCC, MD, USA) and kept them in our laboratory. LNCaP, PC3 and 22RV1 cells were maintained in 90% RPMI 1640 Medium supplemented with 10% fetal bovine serum (FBS) and 1% Penicillin-Streptomycin. C4-2 and C4-2B cells were maintained in DMEM/F12(4:1) Medium and add 10% FBS, 0.100 μg/mL Insulin, 275 ng/mL Triiodothyronine, 88.6 ng/mL apo-Transferrin, 4.9 ng/mL d–Biotin and 251.8 ng/mL Adenine. DU145 cells were maintained in MEM Medium with 10% FBS. All cell lines were cultured at 37°C in a humidified incubator with 5% CO_2. All the medium were purchased from Gibco or Thermo company.

Patient selection and tissue preparation

Fifty-four and Twenty-seven men were enrolled who had been diagnosed with PCa and prostatic hyperplasia with chronic prostatitis between January 2018 and December 2020 in Renmin Hospital of Wuhan university. All patients were Han Chinese and ranged in age from 46 to 82. Cancer tissue, prostatic hyperplasia with chronic inflammation and normal prostate specimens were identified by experienced pathologist and then subjected to immunohistochemical staining, immunofluorescent staining and Western Blot. All samples were from patients who had undergone diagnostic biopsy after screening for elevated PSA, and none of the patients had received finasteride or other treatments related to BPH, and all cancer samples are from primary lesion. The human specimen experiments are accordance with The Code of Ethics of the World Medical Association and approved by the Ethics Committee of Renmin Hospital of Wuhan University, and the protocol number is ChiCTR1800019553. Informed consent was obtained for experimentation with human subjects.

Mice

Six-week-old male nude athymic BALB/c mice (22-30g) were purchased from Charles River Laboratory and were housed in Central Laboratory of Wuhan University People's Hospital, all experiments were carried out in accordance with the National Institutes of Health guide for the care and use of Laboratory animals, as well as approved by the Medical Ethical Committee of the Renmin Hospital of Wuhan University, and the protocol number is WDRM20200904.

METHOD DETAILS

Transfection

The specific shRNA sequence of AICDA or CXCL12 as follows: shAICDA-1 (5′-TGACTTACGAGACGCATTT-3′), shAICDA-2: (5′- TTTC GTACTTTGGGACTTT-3′), shCXCL12-1 (5′-TGTGCATTGACCCGAAGCTAA), shCXCL12-2 (5′-GCCAACGTCAAGCATCTCAAA-3′); and the nonspecific negative control sequence: 5′-TTCTCCGAACGTGTCACGT-3′. Either the specific or the nonspecific sequence contains the gene green fluorescent protein (GFP) to facilitate the filtration of cells with high inhibition efficiency. Briefly, 1000 of experimental cells were planted in a well of 96-well plate and culture by 200 μl of complete media for 24 hours, subsequently, Lentiviral particles and polybrene

in certain volumes were added to the cells at a final multiplicity of infection (MOI) of 100. Replaced with fresh media at 12 hours and continue incubate to72 hours. Western blot assay used to measure inhibition rate. The specific sequence with the best inhibition efficiency was used in the next experiments.

Western blot assay

Briefly, experimental cell deal with trypsin, PBS, RIPA buffer (Beyotime Biotechnology, Shanghai, China), PMSF (Beyotime Biotechnology), PhosSTOP (Servicebio Corporation, Wuhan, China) to obtain protein. Subsequently, appropriate amount of protein along with molecular weight marker (Cat. No. 26617, Page Ruler Prestained Protein Ladder, Thermo) loaded into wells of a 12% sodium dodecyl sulfate–polyacrylamide gel electrophoresis (SDS-PAGE) gel (Biotechwell, Shanghai, China) to perform electrophoresis. Next, the PVDF (Cat. No. 232100, BD Biosciences, USA) membranes were blocked by 5% non-fat milk at room temperature for an hour and subsequently incubated with primary antibodies at 4°C overnight. Secondary antibodies were then incubated for one and a half hours at room temperature. Odyssey infrared imaging system (LI-COR Biosciences, USA) was used to obtain the experiment result.

Immunohistochemistry

Briefly, tissue sections were deparaffinized with xylene and alcohol and then rehydrated by buffer water. Endogenous peroxidase activity was quenched using peroxidase blocking reagent and retrieval solution was used for retrieving antigen. Primary antibody applied was AID Rabbit polyclonal antibody (1:100 dilution, Cat# ab93596, Abcam). Staining of tissue was visualized under a microscope.

Immunofluorescence staining

The PCa tissue sections were fixed in 4% paraformaldehyde and washed three times in PBS. After incubating in blocking buffer (5% BSA), primary antibodies against E-cadherin was added to tissue sections and incubated at 4°C overnight. After rinsing three times with PBS, the tissue sections were incubated with secondary antibodies for 1 h at room temperature in the dark. After washing three times with PBS, the nuclei in the tissue sections were stained with antifade mounting medium including DAPI. Images were acquired under a fluorescence microscope (BX63; Olympus, Tokyo, Japan).

Real-time fluorescent quantitative PCR

Experimental cells were rinsed with phosphate-buffered saline (PBS) twice, then 1 ml TRIzol was added to the lysate cells. The total RNA was extracted according to the manual and its quantity was measured using a UV spectrophotometer. cDNA was synthesized under conditions of 42°C for 40 min and 85°C for 5 min, and used as a template for the amplification of the CXCL12 gene with pre-denaturation at 94°C for 2 min, 30 cycles of denaturation at 94°C for 30 sec, annealing at 60°C for 30 sec and extension at 72°C for 30 sec, then final extension at 72°C for 2 min. The sense and antisense primers of CXCL12 was F: GCTACAGATGCCCATGCCGAT, R: AGCTTCGGGTCAATGCACACT. Following the reaction, the PCR production was identified with electrophoresis in 1.5% sucrose and analyzed with a SensiAnsys gel-imaging system. The expression of mRNA was semi-quantitatively calculated using the optical density ratio of Livin and β-actin. The experiment was repeated three times.

Transwell

Invasion and migration assay was realized by Transwell plates coated with (or without) Matrigel Matrix at a 1:8 dilution ratio. The cells at a concentration of 1×10^5 (or 0.5×10^5) cells in 100 μl non-FBS medium were planted in the upper chamber and 600μl medium containing 20% FBS was seeded in the lower chamber. Incubate in cell incubator at 37°C with 5% CO_2 for 48 hours, and 4% paraformaldehyde and 0.05% Crystal was used to immobilize and stain the cells. The number of invasion cells was counted under a microscope.

CCK-8 assay

Cell proliferation assay was performed utilising the CCK-8 in accordance with the manufacturer's instructions (MedChemExpress, Cat #HY-K0301). Briefly, experimental cells were inoculated in a 96-well plate to investigate the effect of AID on cell proliferation. At time points of 0, 24, 48 and 72 h, 96h, 120h, 144h, and 10 μl of WST reagents were added per well, and the cells were incubated for 60 min. Absorbance was then measured at 450 nm by using a multilabel counter (Perkin Elmer, Singapore).

Animal experiment

In tumorigenesis assay, cells were treatment with 0.25% trypsin-EDTA solution and rinsed in Hank's balanced salt solution (HBSS). 5×10^6 cells per 100 μl solution was injected subcutaneously into male nude athymic BALB/c mice (six-week-old) (n = 8). Tumor volume (in mm^3) was calculated by the formula 0.5 × (long diameter) × $(\text{short diameter})^2$. In metastasis assay, cells at a concentration of 2×10^6 cells per 200 μl HBSS were injected intravenously into the tail vein of nude mice (n = 8). All the mice were sacrificed by CO_2 overdose transiently after 14 days. Next, lung samples were used in IHC and HE staining. Image-Pro Plus 6.0 was used to observed the experiment result. In survival assay, 4×10^6 cells per 200 μl HBSS were injected intravenously into the tail vein of nude mice (n=17). Kaplan-Meier Curve was established to estimate the survival among experiment and control group.

QUANTIFICATION AND STATISTICAL ANALYSIS

All experiments repeat at least three times. Image J software is used to measure the expression of target proteins in WB, IHC or IF assay. Data were shown as mean ± standard deviation. One-way ANOVA or Student's t test was used in Western Blot, IHC, immunofluorescent staining and transwell assay, as well as in animal experiment. Log rank was performed on survival analysis. Pearson correlation coefficient was used in gene correlation analysis. All dates are processed by SPSS 23.0 (IBM, USA) and Statistical significance was defined as *$P<0.05$, **$P<0.01$, ***$P<0.001$.